



NTNU – Trondheim
Norwegian University of
Science and Technology

Experimental study of displacement of viscous oil in pipes by water

Milad Kazemihatami

Natural Gas Technology

Submission date: July 2013

Supervisor: Ole Jørgen Nydal, EPT

Co-supervisor: Zhilin Yang, EPT

Norwegian University of Science and Technology
Department of Energy and Process Engineering

EPT-M-2013-66

MASTER THESISFor
Stud.techn.Milad Kazemihatami

Spring 2013

Experimental study of displacement of viscous oil in pipes by water*Forsøk med fortrenning av viskøs olje med vann***Background**

One of the main issues of long distance transport of offshore multiphase viscous crude is how to restart the production after un-expected shut-in of the flowline. If the fluid mixture is transported in terms of water continuous flow under normal production condition, during shut-in, the oil and water will separate, and form many oil or water columns in the flowline of un-even topology. At the same time, the fluids will be cooled down, and eventually the fluid temperature will reach sea bottom temperature, which gives extremely high oil viscosity. The complete displacement of these cold oils is needed before the production of oil is resumed.

A correct prediction of the displacement of oil column of multiphase viscous flowline after shut-in is essential for the pipe line design and for effective operation. The classical multiphase flow codes assume plug flow, therefore it gives too conservative prediction of the restart time. There is a need to understand the physical process of propagation of interfaces of oil and water columns during the restart process at different pipe geometry.

Objectives

Perform experimental study on the flushing process of different combinations of oil and water columns at different pipe geometry: inclined, V and W shape, etc. The experiments should be able to provide transient information of interface movement.

The following tasks are to be considered

- 1 A short literature search on displacement of viscous oil column by water
- 2 Laboratory preparation and instrument calibration
- 3 Pipe flow experiment with different pipe geometry and different flushing flow rates of water
- 4 Data analysis, and quantification of complete displacement process.
- 5 Suggestions for further work

Preface

This thesis report has been performed at the Norwegian University of Science and Technology (NTNU) in the course of spring 2013.

For most of the time I have been working at NTNU multiphase laboratory, in order to prepare the setup and conduct desired experiments. As well as the experiments, I spent some time at Department of Energy and Process Engineering of NTNU for running simulation with LedaFlow® and analysis the experimental output data and process the data to conclude this report.

Many people have been of great help during this research period. First and foremost, I would like to thank my supervisor at NTNU Ole-Jørgen Nydal for giving me an opportunity to do both experimental and simulation work and for the great guidance during this work. I wish also to thank Statoil AS – Flow Assurance R&D Department for supporting this research project and specially my co-supervisors, Zhilin Yang who is also giving me his guidance and support. I would like to express special thanks to Mariana J.C. Diaz, Heiner Schümann and Tienan Yin for their help, guidance and cooperation during the test period. It has been fun and challenging to work with them. In the multiphase laboratory at NTNU, Paul Svendsen and Martin Bustadmo have skillfully participated to the construction of the jumper setup.

Finally, I am grateful to my fellow Master students at the Energy and Process Technology Department for the nice atmosphere, the help and the suggestions they provided me during the period.

Trondheim, July 2013

Milad Kazemihatami

Abstract

This study is specifically concerned with the understanding of real restart procedure that is very crucial for prediction of oil-water columns displacement after un-expected shut down at water-viscous crude oil transportation. This issue gets more important for subsea pipeline which is generally located in ups and downs topology and in average cold medium. At subsea pipelines the risk of formation of oil-water columns is high and in addition the viscosity of crude oil gets higher due to heat transfer with sea water.

The present study has reported the experimental activities carried out to investigate of viscous oil displacement in pipes by water. Basic aspects regarding oil-water flow, viscosity of crude oil and flow assurance have been reviewed initially. The tests were established at the acrylic transparent 60-mm internal diameter pipe at horizontal/inclined test rig and in the small-scale of M-shaped jumper. In addition, a series of simulations have been run in LedaFlow® 1D. The experimental setup has been designed and constructed at NTNU multiphase laboratory. The setup was prepared for movable visual capturing such that a series of lightening and camera carrier have been installed. A total of 56 individual experiments were conducted and the measurements were made for different oil and water flow rate in horizontal and inclined pipe line. Some tested cases were simulated LedaFlow® 1D and results are compared.

Both qualitatively and quantitatively results of the experiments and observation from displacement tests have been documented in this report. Most of outcomes indicate that the front of shape of propagation interface is changing along the pipe. Droplets accumulation and wavier interface have been observed at the end section of the pipe in compare to beginning section. By experimental analysis was found that the minimum superficial velocity of water in order to remove all residual oil at M-shaped jumper is around 0.38 m/s. Concerning LedaFlow® 1D simulation efforts, the front shape prediction for number of tests was running and corresponded results have been stated.

Nomenclature

Latin letters

A	Cross-sectional area [m ³]
D	Pipe diameter [m]
F	Shear force [N]
f	Friction factor [-]
g	Gravity coefficient [m/s ²]
H	Water Volume Fraction (Water hold up) [-]
P	Pressure [bar]
Q	Mass flow rate [Kg/s]
S	Wetted periphery [m ²]
s	Slip ratio [-]
U	Velocity [m/s]
V	Volume [m ³]

Greek letters

α	Phase volume fraction [-]
λ	Phase volumetric flow rate fraction [-]
ξ	Inclination Degree [rad]
μ	Absolute viscosity [cP]
τ	Share stress [Pa]
ϑ	Kinematic viscosity [m ² /s]

Abbreviations

1D	One Dimensional
CFL	Courant–Friedrichs–Lewy condition
CV	Control valve
GVF	Gas volume fraction
LEDA	A multiphase flow simulator
PIP	Phase inversion point
PLEM	Pipeline end manifold
PLET	Pipeline end termination
RHS	Rectangular hollow ection
V	Valve

Subscripts

i	Initial
m	Mixture
o	Oil
S	Superficial
w	Water

Contents

Preface.....	iii
Abstract	v
Nomenclature.....	vii
Contents.....	ix
1 Introduction.....	1
1.1 Background.....	1
1.2 Objectives and Scope of work	1
1.3 Tools used.....	2
1.4 Report Structure.....	2
2 Theory	3
2.1 Flow Assurance	3
2.2 Problems related to viscose oil transportation.....	3
2.3 Crude oil viscosity	4
2.3.1 Effect of Temperature on oil viscosity.....	5
2.4 Two phase Oil-water flow	6
2.4.1 Basic definitions	6
2.4.2 Oil-water flow regimes and flow pattern maps	6
2.4.3 Phase inversion.....	8
2.4.4 Oil-water flow pattern dependent prediction models.....	9
2.5 Subsea connections and jumpers	10
2.6 LedaFlow1D, multiphase simulation tool	12
3 Experimental Setup and Methodology.....	13
3.1 Small-scaled M-shaped jumper setup.....	13
3.1.1 Overview and design consideration	13
3.1.2 Main dimension of the rig	16
3.2 Horizontal rig setup	17
3.2.1 Overview and main dimension of rig.....	17
3.2.2 Additional start and end section	18
3.2.3 Air Release valve.....	18
3.2.4 Cameras setup (stationary and movable).....	19
3.2.5 Lightening system	19
3.2.6 Anti-reflection cover	20
3.2.7 Pressure transducer and calibration procedure.....	21

3.2.8	Conductance probe and calibration procedure	22
3.3	Oil-water front experiment at horizontal and inclined pipe	24
3.3.1	Oil bubble flushing with water at inclined test section	24
3.3.2	Fully filled oil pipe flushing with water at inclined test section	24
3.3.3	Fully filled oil pipe flushing with water at horizontal test section	24
3.3.4	Fully filled water pipe flushing with oil at horizontal test section	24
3.4	Oil-water flushing test in M-shaped jumper test	25
4	Results of Experiments and Discussion	26
4.1	Oil bubble flushing with water at inclined test section	26
4.2	Fully filled oil pipe flushing with water at inclined test section	28
4.3	Fully filled oil pipe flushing with water at horizontal test section	30
4.4	Fully filled water pipe flushing with oil at horizontal test section	32
4.5	Oil-water flushing test in M-shaped jumper test	34
5	Simulation of experimental cases, results and discussion	36
5.1	Construction of the case	36
5.1.1	Flow path geometry and meshing	36
5.1.2	Fluid properties	37
5.1.3	Boundary Condition	37
5.1.4	Initial Condition	37
5.1.5	Numerical setting	38
5.2	Oil-water front simulation results	38
6	Conclusions and recommendation for further works	40
7	References	42
Appendices		43
Appendix A		43
Appendix B		46
Appendix C		47
Appendix D		48
Appendix E		52
Appendix F		55
Appendix G		58
Appendix H		61

1 Introduction

1.1 Background

Due to higher demand of energy, production of hydrocarbons has been increased. Transportation of this resource with pipeline is included at energy value chain. Oil-water mixture is content of transportation pipeline in some offshore and onshore fields. Shut down of hydrocarbon transportation is happened time to time due to technical problems and other operational issues. In order to resume the fluids transportation some issues occur frequently. For instance, forming of viscose oil and water columns causes trouble for the flow restarting. Viscose oil columns within pipeline should remove at the beginning of the restart procedure.

Efficient operation of pipeline and even design of flow lines require to understanding of true oil column displacement prediction. The viscous oil column has been considered as a rigid plug in the classical multiphase codes. The experimental results concerning process of propagation of interfaces of oil - water columns are valuable for better prediction. The shape of front part of oil or water propagation can be significant phase of this investigation. Series of experiment have been conducted concerning models evaluation.

Oil spill during subsea intervention is another issue which should be considered for subsea flow path such as jumpers within offshore production systems. Mainly water injection through, so-called, service line is common way to replace oil before disconnecting of the pipes at the sea bed. Minimum superficial velocity of water in order to displacement of all residual oil in such a complicated configuration jumpers is crucial to meet operation standard requirements. The qualitatively flushing description and oil-water front propagation estimation will be introduced at this dissertation effort.

1.2 Objectives and Scope of work

Conducting series of experiment in order to investigate of viscous column oil-water flushing have been our main objective. The tests have been run at various pipe geometries such as horizontal and inclined, with different flow rate injection and initial condition. The results show the transient behaviour of interface movement along the pipe.

Another objective was to find the minimum water injection superficial velocity in order to removing all residual oil in special flow line configuration (jumper geometry) and finding the front shape estimation by both experiment and simulation.

1.3 Tools used

The experimental purpose of our work was conducted at the NTNU multiphase flow laboratory. The laboratory is equipped with two relatively large centrifugal pumps for oil and water, two relatively small centrifugal pumps for oil and water, two screw pumps, separator tank, horizontal loop pipes and control panel. Two stationary cameras and one movable camera were used during the experiment.

LedaFlow® was a multiphase flow simulator which has been used during this project. Leda considers flow as three phase fluid; water, oil and gas. Each phase could be continuous or dispersed to other phase. [1]

1.4 Report Structure

The report starts with introduction in chapter 1. Chapter 2 will introduce the fundamental theory of viscous oil flow assurance problem and basics of oil-water flow. Chapter 3 provides descriptions of the experimental efforts included setup description and tests procedure. Chapter 4 offers the results and discussion of the experiments. Chapter 5 deals with simulations work and the results. The last section is conclusions and recommendation for further works. The supplementary information is placed in the appendixes.

2 Theory

This chapter provides an introduction of the fundamental theory of viscous oil flow assurance problem and basics of oil-water flow.

2.1 Flow Assurance

Flow assurance offers technical solutions at reasonable costs, environmentally and without risk to design and operate transportation through all flow lines and pipelines from reservoir to onshore process plants [2]. Flow assurance is a concept which is followed by the transportation of multiphase flow; mostly in offshore pipelines. Transportation of oil, gas, liquid and water simultaneously in flow lines and pipelines can have some operational problem [3]. Therefore the correct handling of flow assurance is critical for successful operation.

The main problems which can occur in the multiphase transportation are: [4]

- Hydrate formation
- Deposition of wax and asphaltene (problems for pigging operation).
- Scale formation
- Corrosion
- Erosion
- Severe slugging (dangerous for downstream processes)

2.2 Problems related to viscose oil transportation

Demand of oil increase globally. **Figure 2-1** is shown the oil consumption of world by 2020 [5]. In addition, 70% of oil reserves in the world are heavy oil with high viscosity [6]. The viscosity of the light oil will be also increase due to heat transfer from oil.

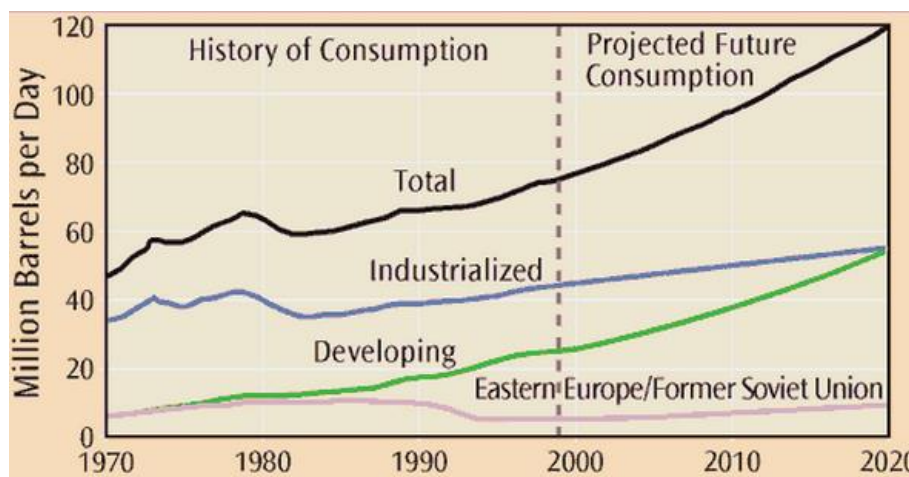


Figure 2-1: World oil consumption by region 1970 - 2020

In order to transport viscous oil through pipe line some methods are frequently used in oil industry, like:[7]

- Heating
- Dilution
- Oil water emulsion
- Core annular flow
- Partial field upgrading

Mixture of oil and water in design operation run without major problem. At undesirable shut down, oil and water separate from each other and form the columns in up and down sections. **Figure 2-2** shows the shutdown procedure.

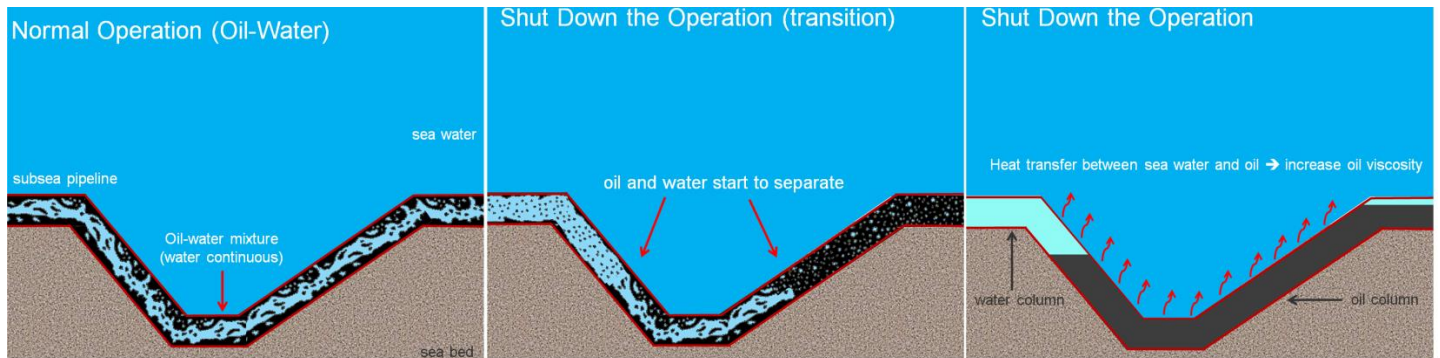


Figure 2-2: Oil and water column formation in subsea pipeline

2.3 Crude oil viscosity

Viscosity is described as the internal resistance of the fluid to flow and it is one of the main governing properties of the fluid [8]. Generally fluid viscosity is divided into two main categories, absolute viscosity and kinematic viscosity. Absolute viscosity is shearing force per unit area of moving surface per velocity of moving surface, and Kinematic viscosity is absolute viscosity divided by mass density [9]. The main equations (Equation 2-1 and Equation 2-2) regarding viscosity are introduced here:

$$F = \tau A = \mu A \frac{du}{dy} \quad \text{Equation 2-1}$$

$$\vartheta = \mu / \rho \quad \text{Equation 2-2}$$

Where F (N) is shear force, τ (Pa) is shear stress, A (m^2) is area, μ^1 (cP) is absolute viscosity and ϑ (m^2/s) is kinematic viscosity. There is many ways and correlations introduced in order to estimate crude oil viscosity. Some correlations such as: Beal, Vasquez and Beggs, Khan, and Kartootmodjo and Schmidt [10].

¹ 1 cP = 1 mPa·s = 0.001 Pa·s

2.3.1 Effect of Temperature on oil viscosity

Many experimental results and also modeling works show the rheological behavior of crude oil at various temperatures. For instant, the **Figure 2-3** shows the result of temperature effect (0-60°C) on viscosity value for 27 different crudes. This clearly indicates that by decreasing the temperature, viscosity value will increase dramatically. The maximum viscosity difference is almost 100 KcP. In simple word the crude oil convert to solid in low temperature. [11]

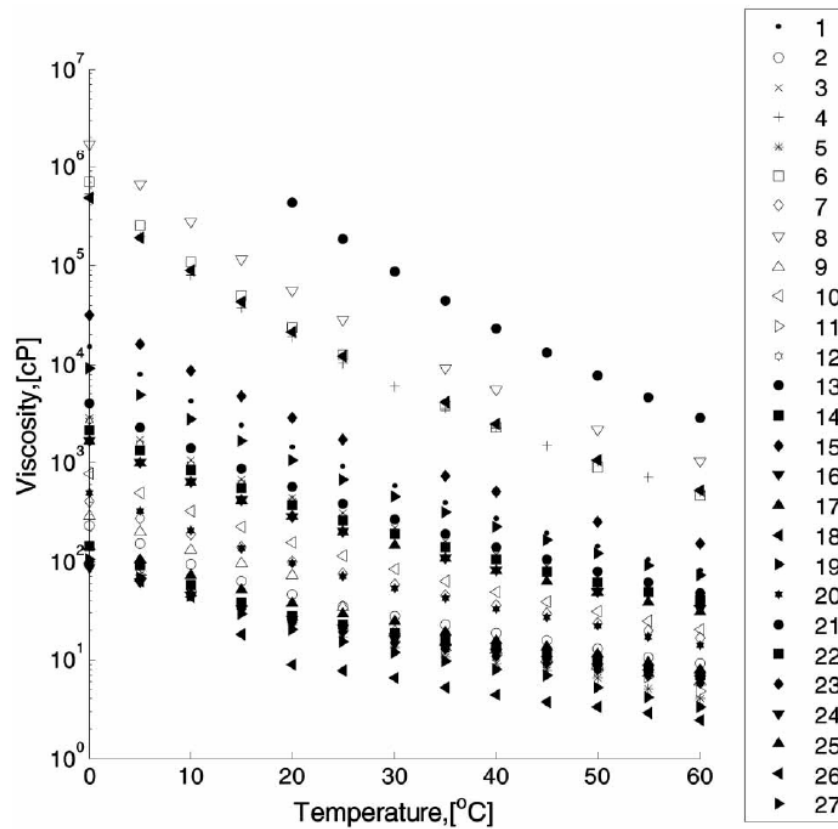


Figure 2-3: Viscosity as a function of temperature for 27 various crudes oil[11]

2.4 Two phase Oil-water flow

In this section, an overview of the existing studies on oil-water flow will be reviewed in brief and some issues related to that term will be discussed. Basic definitions, flow patterns and relevant maps and prediction flow models, especially on steady-state flows, are in focus.

2.4.1 Basic definitions

Assume oil-water flow in a pipe with cross-sectional area A . Q_w and Q_o are input water and oil volumetric flow rate, respectively. The volumetric flow rate fraction for water and oil are given by [12],[13] :

$$\lambda_w = \frac{Q_w}{Q_w + Q_o} \quad \text{Equation 2-3}$$

$$\lambda_o = \frac{Q_o}{Q_w + Q_o} \quad \text{Equation 2-4}$$

Here λ_w is also used as the term water cut in oil-water occasionally, particularly in flow applications. The volume fraction (α) for water and oil respectively is defined as:

$$\alpha_w = \frac{A_w}{A} \quad \text{Equation 2-5}$$

$$\alpha_o = \frac{A_o}{A} \quad \text{Equation 2-6}$$

The superficial velocity and the actual velocity for oil and water phases can be calculated as follows:

$$U_{SW} = \frac{Q_w}{A} \quad U_w = \frac{Q_w}{A_w} \quad \text{Equation 2-7}$$

$$U_{SO} = \frac{Q_o}{A} \quad U_o = \frac{Q_o}{A_o} \quad \text{Equation 2-8}$$

The slip ratio (S) is applied as a relation between the two phases actual velocity and is defined as:

$$s = \frac{U_o}{U_w} = \frac{A_w U_{SO}}{A_o U_{SW}} \quad \text{Equation 2-9}$$

If the slip ratio is greater than 1, means that the oil flows faster than water; while if s is less than 1, shows that the water is the faster phase. Same phases velocity is indicates $S=1$. The slip ratio is affected by the phases' physical properties, the flow pattern, the flow rate and the pipe geometry.

2.4.2 Oil-water flow regimes and flow pattern maps

In oil-water flow, various internal flow structures and spatial distributions of their deformable interface can occur. These shapes are commonly called flow regimes or flow patterns. Knowledge of the flow

regimes in certain condition could be helpful for better predicting oil-water flow behavior. A large number of experiments have been conducted in order to investigate flow patterns under given conditions. The influence of pipe diameter, geometry and oil viscosity on the flow pattern has been investigated by [12]. The interfacial structures for oil-water flow (patterns) are classified by many people in different ways. One possible classification for horizontal flow is shown in **Figure 2-4** by Trallero et al (1997) [14]. The **Figure 2-5** gives another classification of oil-water patterns in vertical pipe (106.4 mm) which are carried out by Abduvayt et al [15]. The flow patterns are divided in to main categories: Water dominated and oil dominated. The flow pattern maps are generated by results of observation. Here, two flow patterns are shown in **Figure 2-6-b** for horizontal and **Figure 2-6-c** for vertical pipe geometry at different gas and liquid superficial velocities.

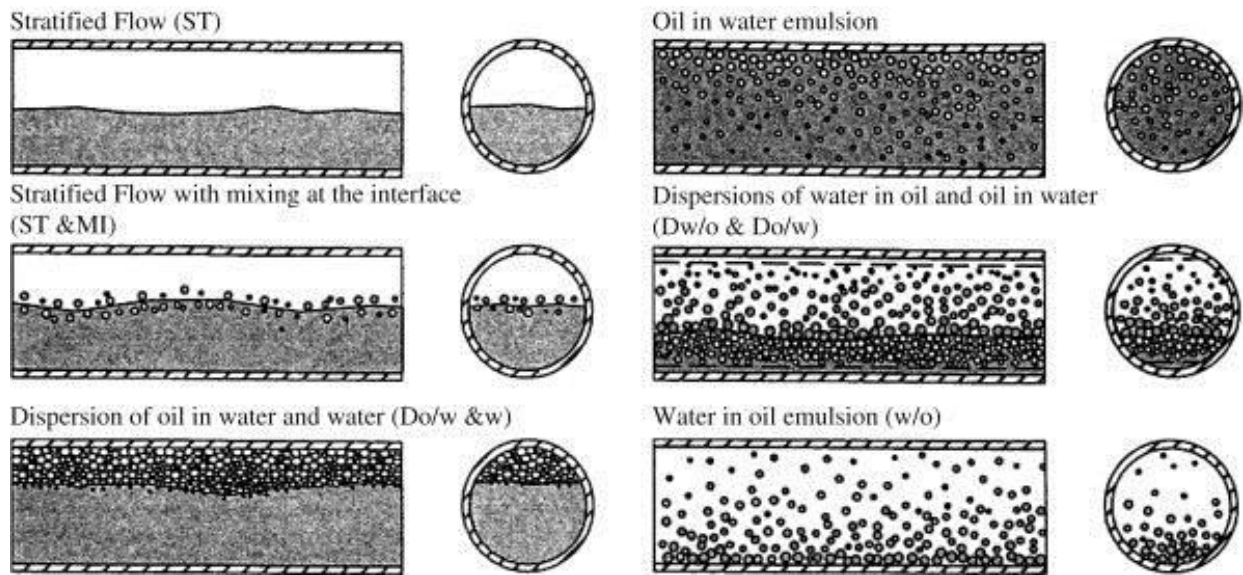


Figure 2-4: Horizontal oil-water flow patterns [14]

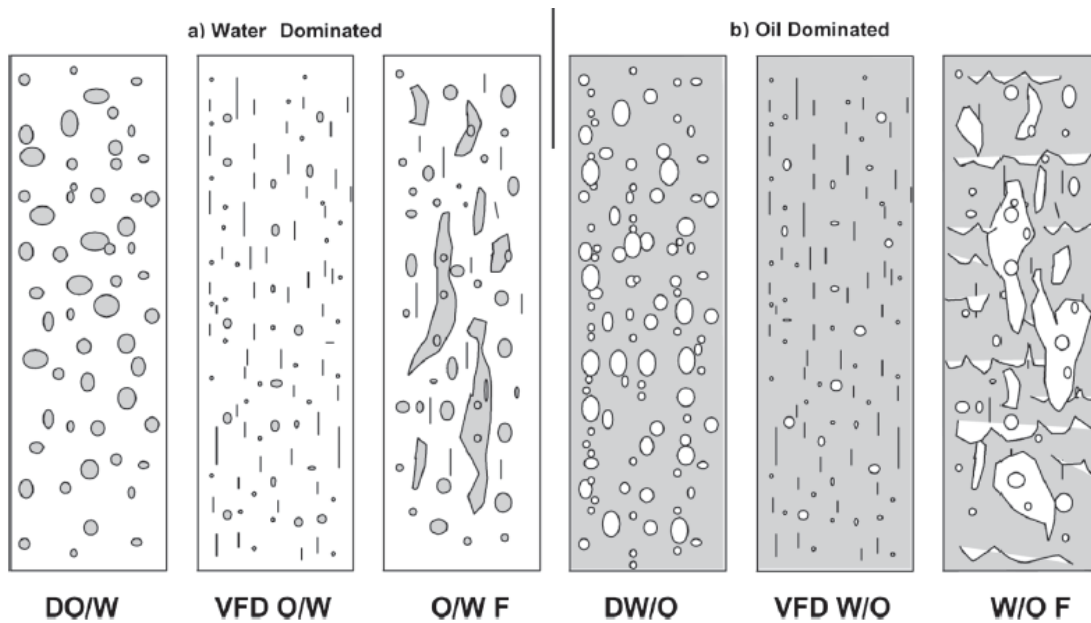


Figure 2-5: Vertical oil-water flow pattern [15]

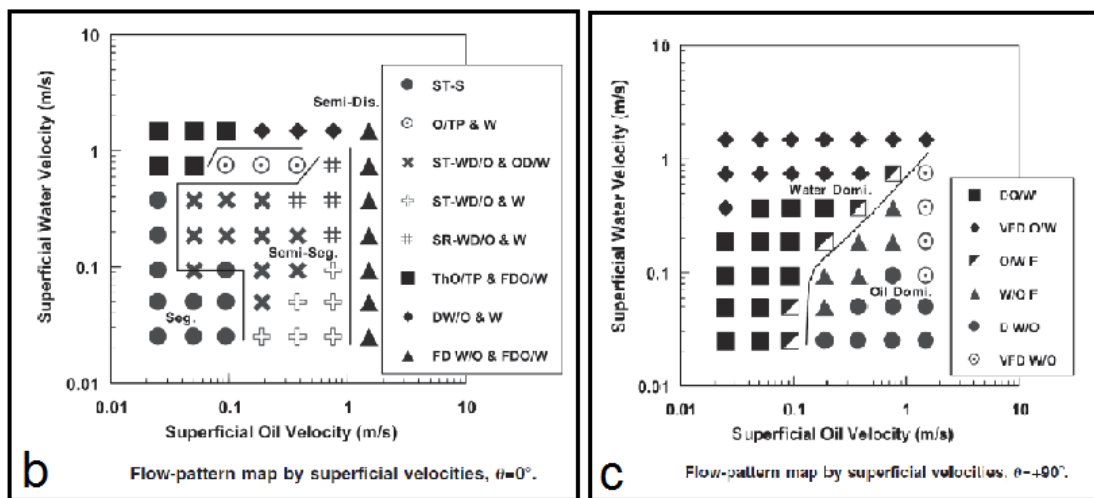


Figure 2-6: Flow pattern map [15]

2.4.3 Phase inversion

Phase inversion occurs when a dispersion of oil in a water continuum becomes dispersion of water in oil continuum or vice versa. The inversion occurs normally within a narrow band of change in the operational conditions. Phase inversion causes a sudden change in heat and mass transfer between the phases and rate of momentum due to change of continuous phase. A critical result associated with phase inversion is a dramatic change of pressure drop. PIP is defined as the phase inversion point. **Figure 2-7** gives the phenomenon process. Here, it is indicated that at PIP the phase inversion occurs and the pressure drop reduces. PIP is one a significant criteria in the design of transportation pipe lines. Therefore operators have to ensure that sufficient water or oil volume fraction is available during operation [12], [16].

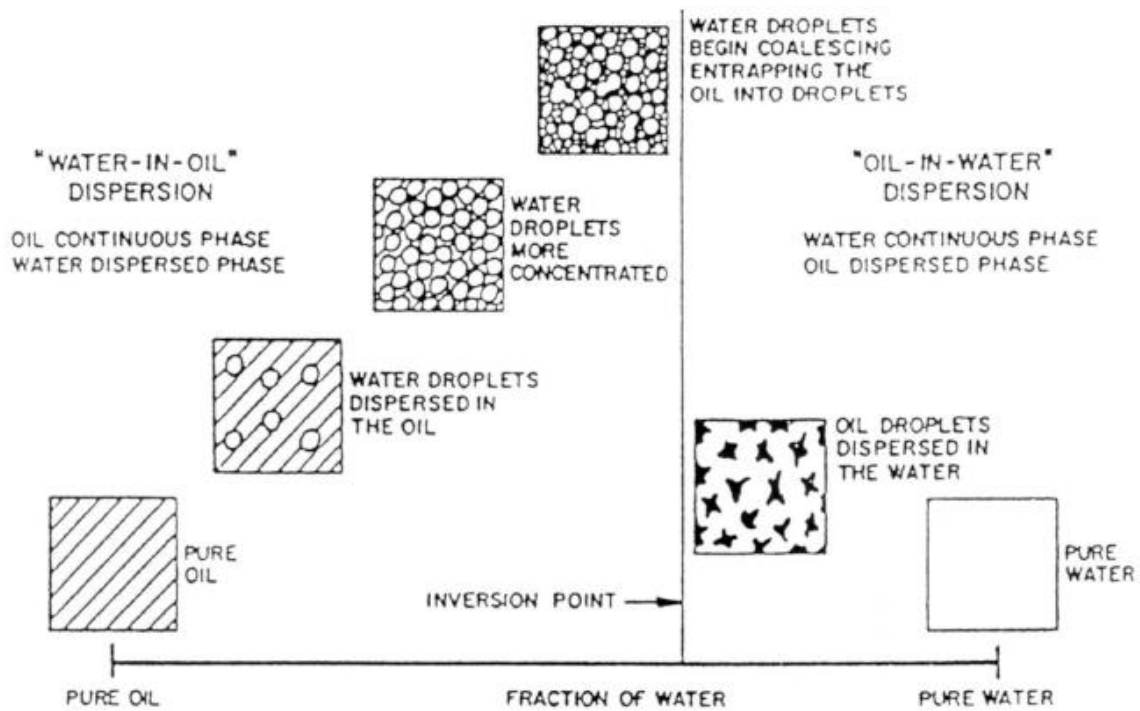


Figure 2-7: The phase inversion process [16]

2.4.4 Oil-water flow pattern dependent prediction models

Oil-water flow could be divided into two main categories of flow pattern: stratified and dispersed oil-water flow. The available mechanistic models have been developed based on the expression of the dominant physical mechanism of the flow process. For separate flow (stratified flow) it is very common to use one dimensional two fluid balance for each phase. The momentum balanced equation for oil and water phase is derived as follow [12], [17], [18]:

$$A_w \left(\frac{dp}{dx} \right) - \tau_w S_w - \tau_i S_i - \rho_w A_w g \sin \xi = 0 \quad (\text{Water phase}) \quad \text{Equation 2-10}$$

$$A_o \left(\frac{dp}{dx} \right) - \tau_o S_o + \tau_i S_i - \rho_o A_o g \sin \xi = 0 \quad (\text{Oil phase}) \quad \text{Equation 2-11}$$

Where, A_w and A_o are the area of cross-section for water and oil, respectively. Pressure gradient is presented by dp/dx . τ_o , τ_w , and τ_i are the wall share stress for oil, water and interfacial share stress, respectively. S_o , S_w and S_i is wetted periphery for oil-wall, water-wall and interfacial phases, respectively.

Here, many empirical correlations have been established to predict wall and interfacial share stress.

For dispersed oil-water flow the most common prediction model is the homogenous no-slip model. In this method, mixture of a fluid is considered as a “pseudo-fluid” with average mixture properties. The pressure gradient homogenous model is given by:

$$\frac{dp}{dx} = \frac{f_m \rho_m U_m^2}{2D} - \rho_m g \sin \xi \quad \text{Equation 2-12}$$

Where D is pipe diameter, f_m is mixture friction factor. ρ_m and U_m are mixture density and velocity, respectively. The mixture velocity is calculated by:

$$U_m = U_{SO} + U_{SW} \quad \text{Equation 2-13}$$

The mixture density can be determined as follow:

$$\rho_m = \alpha_w \rho_w + \alpha_o \rho_o \quad \text{Equation 2-14}$$

2.5 Subsea connections and jumpers

Jumpers in subsea production system are defined as rigid or flexible flow lines between subsea components such as X-mas tree, manifold, PLEM, PLET and export sled. The length of the jumper is relatively short and it can be used as pipe for injecting water or chemicals to the well when production fluids are used. In technical terminology, jumpers are categorized as subsea tie-in system. **Figure 2-8** shows a typical subsea jumper system. Since the jumper geometry normally has not any thermal insulation and because of its shape which has low a spot in flow line where free water can accumulate the risk of Hydrate formation raises. Therefore, studying of flow assurance aspects in this component is of major importance for oil and gas industry. [19]

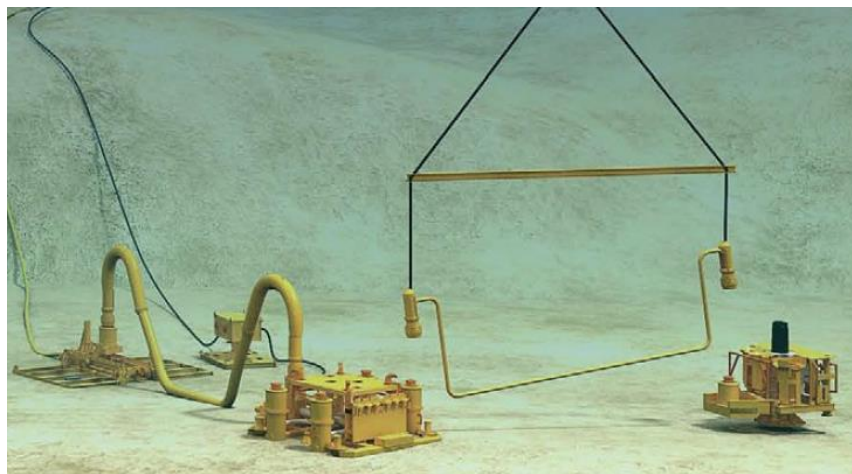


Figure 2-8: Subsea jumper systems [19]

Jumpers typically have two end connectors and a flow pipe line between the connectors. Based on the construction material, jumpers are also divided into rigid and flexible types. The flexible type has no special configuration, but the rigid types have some well-known configuration. M-shaped style (both normal and elbow), inverted U-shaped and Z-shaped which is frequently utilized in horizontal jumpers. **Figure 2-9** show some of these configurations. [19]

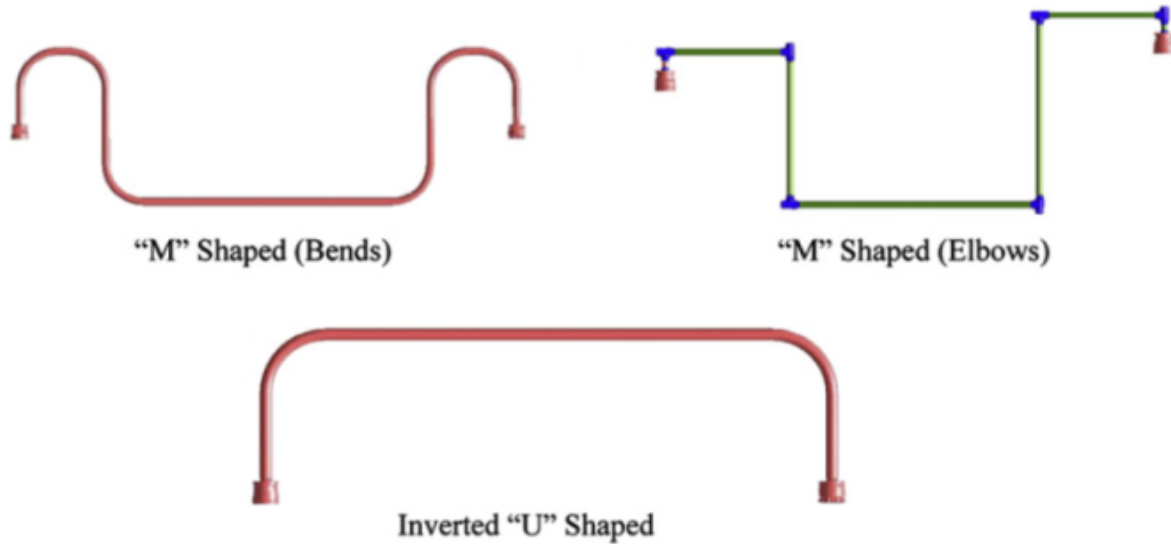


Figure 2-9: Rigid jumper configurations [19]

Jumpers are often fabricated after the subsea component has been installed at the sea bed. Then the geometry and distance between the components are measured or calculated In order to provide the supplier with information needed. [19] In the experiment, a lab-model was built which mimics the typical M-shaped jumper. The M-shaped type inherently has a high risk of oil spill due to a low spot volume.

In subsea intervention, the retrievable components are replaced frequently. The residual hydrocarbon in connection such as jumpers should be evacuated before disconnect at seabed. The residual oil connections will be discharged into sea water during replacement. The oil companies must prevent discharge of oil in the sea water in order to meet the operation standard such as OSPAR convention and KLIF (Klima- og forurensningsdirektoratet) requirements.[20]

2.6 LedaFlow1D, multiphase simulation tool

Leda is a multiphase flow simulator which is released recently (version 1.1 January 2012). In Leda, the approach is to upgrade accuracy by implementing more fundamental physics. The capability of the simulator is improved by tuning correlation with experimental and field data (SINTEF and TOTAL) [21].

Leda considers flow as three phase fluid, water oil and gas. Each phase could be continuous or dispersed to other phase. For instant, water may be continuous flow, or dispersed as bubble in oil or in gas. Therefore nine phases could be defined as done in Leda. **Figure 2-10** gives a schematic of applied models in Leda.

The fields are characterized by composition, volume fraction, velocity, viscosity and other fluid properties. The flow simulate by solve equations numerically. Thus Leda offers heat and mass transfer models. In addition LedaFlow® provides some option to add source, valve, bends, pig and slug tracking for more complicated case.

The experimental cases were constructed in LedaFlow® 1D and the results were compared.

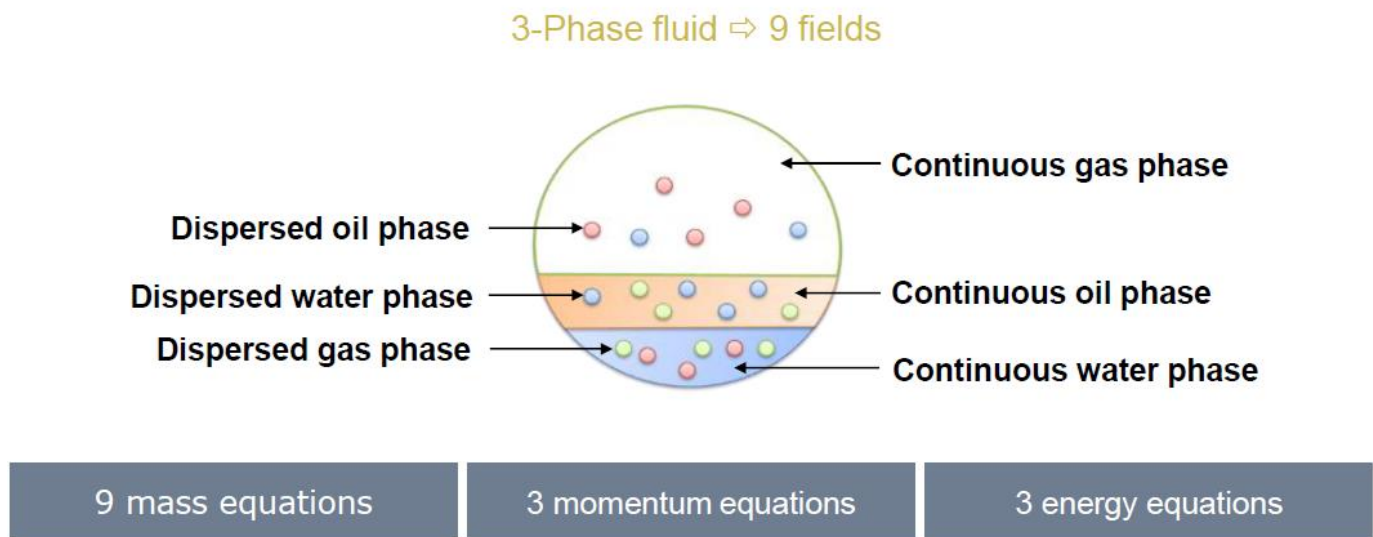


Figure 2-10: View of multiphase flow model in Leda [22]

3 Experimental Setup and Methodology

The purpose of this chapter is to present experimental activities which have been done at NTNU multiphase flow laboratory. In section 3.1, small-scaled M-shaped jumper test and relevant issues are mentioned. In section 3.2, the horizontal rig test will be discussed. The tests procedures of oil-water front shape prediction and the water-oil experiment at the jumper is described in details in sections 3.3 and 3.4 respectively. The results, qualitatively description of the flushing process and sweep efficiency are parts of this section.

3.1 Small-scaled M-shaped jumper setup

In this section, design of the experimental setups for small-scaled M-shaped jumper will be reviewed. Design consideration and constrains issues is also mentioned.

Since our objective is studying on oil-water flushing based on special geometry of jumpers, therefore it was tried to make the experiment setup mimic to typical subsea jumper. M-shaped jumper was selected and the Lab-model has been made with some consideration regarding loop and material constrains. Because the experiment setup was connected to the multiphase flow lab loop, first the laboratory loop is brief described and then the main setup and design consideration is explained afterwards.

3.1.1 Overview and design consideration

The three-dimensional overview of the multiphase flow rig is shown in **Figure 3-1**. The flow loop is consist of air, water and oil supply. The whole system is placed at two levels. Large three phase separator, Oil and water pumps and Air pressure supply tank is placed at basement and flow lines continue to lab-level and all flow meter, control valve, horizontal test section and S-riser are placed this level. The flow line of test was connected to a mixer/inlet section containing the air/water/oil supply. The main fluid properties are listed briefly at **Table 3-1** which is calculated at 1 atm. and 20°C. The outlet section of flow lines are connected to the atmospheric separator, therefore all properties are calculated in 1 atm.

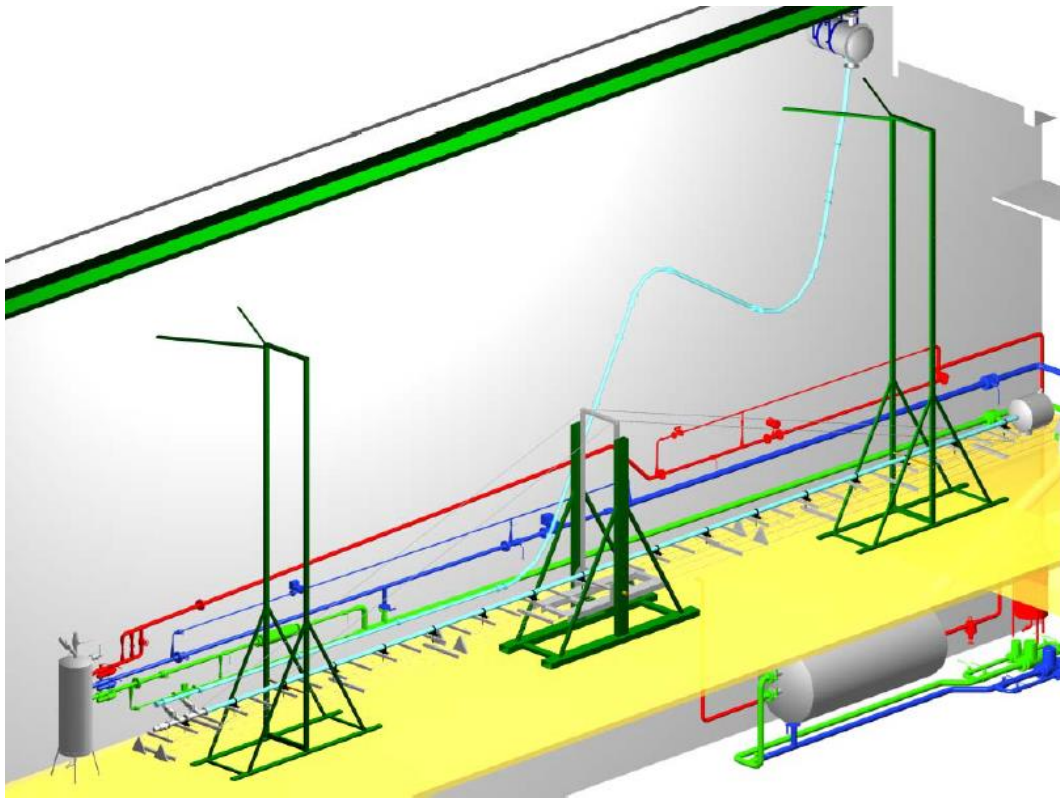


Figure 3-1: Multiphase test rig layout, NTNU [23]

Table 3-1: Fluid physical properties[23]

Physical property	Air	Water	Oil (Exxsol D80)	NEXBASE® 3080
density, kg/m³	1.20	1000 +/- 0.2%	800 +/- 0.2%	840 +/- 0.2%
viscosity, Pa.s	$1.8 \cdot 10^{-5}$	$1.11 \cdot 10^{-3}$ +/- 1.2%	$1.79 \cdot 10^{-3}$ +/- 1.2%	$90 \cdot 10^{-3}$ +/- 1.2%
surface tension, N/m	-	0.0608 +/- 0.0005	0.0246 +/- 0.0005	-

The main experimental setup is the small-scaled of a rigid M-shaped subsea jumper which was frequently used. This kind of jumper consists of vertical and horizontal parts, 90 degree bends and 180 degree bends which looks like two humps. Some of the design consideration and limitation for the setup are listed below:

- The setup mimic to desired jumper geometry.
- The flow line is transparent (semi-transparent) for capturing.
- The pipe inlet diameter is not less than 50 mm.
- The curves radius of bends should not be more than 1 meter due to lab-space limitation.
- The setup can connect to the mail loop in order to supply oil, water and air.
- The flow lines should be fixed to avoid vibration and effect to experiment and capturing.

Since part of the experiment was studying the different points of flow line; the pipe has to be transparent. On the other hand, Setup has some bends along the flow lines which limit our option. Two main choices were considerable: Plexiglas (acrylic) standard pipes or transparent hose. The problem of Plexiglas was absence of standard bend. Therefore in order to utilize the Plexiglas as flow path it should be ordered desired bends to suppliers. Making Plexiglas bend needed considerable time and money. Second option was to implement hoses. The hose can shape easily, however it needs support to keep its shape. The other issue regarding hose is limitation for bending. All hose suppliers recommend a minimum radius for each particular hose to avoid diameter change along bending. This limitation is less when spring reinforced hose is utilized. For example with the same inlet diameter (60 mm), the recommended minimum bend radius for without spring is 700 mm while it is 50 mm for reinforced hose. However, the reinforced hose has less transparency rather than fully transparent hose but it has acceptable for the experiment purpose. Therefore the reinforced hose with inlet diameter 50 mm has been chosen.

As it mentioned before, the hose needs rigid support to keep its shaped. For supporting the horizontal and vertical sections the steel beam structure was utilized. The hose connected to the beam with wire tie as can be seen from **Figure 3-2 a**. The most critical part was 180° bend. For making this part of our support, first the steel 50 x 20 mm RHS profile was bended by using the steel bending machine, see **Figure 3-2 b**. Then mount the fit pipe clamps along the bend as shown in **Figure 3-2 c**. Two 180° bend support was made with same dimension. After wards both bends was mounted at same level to the vertical support of the rig.

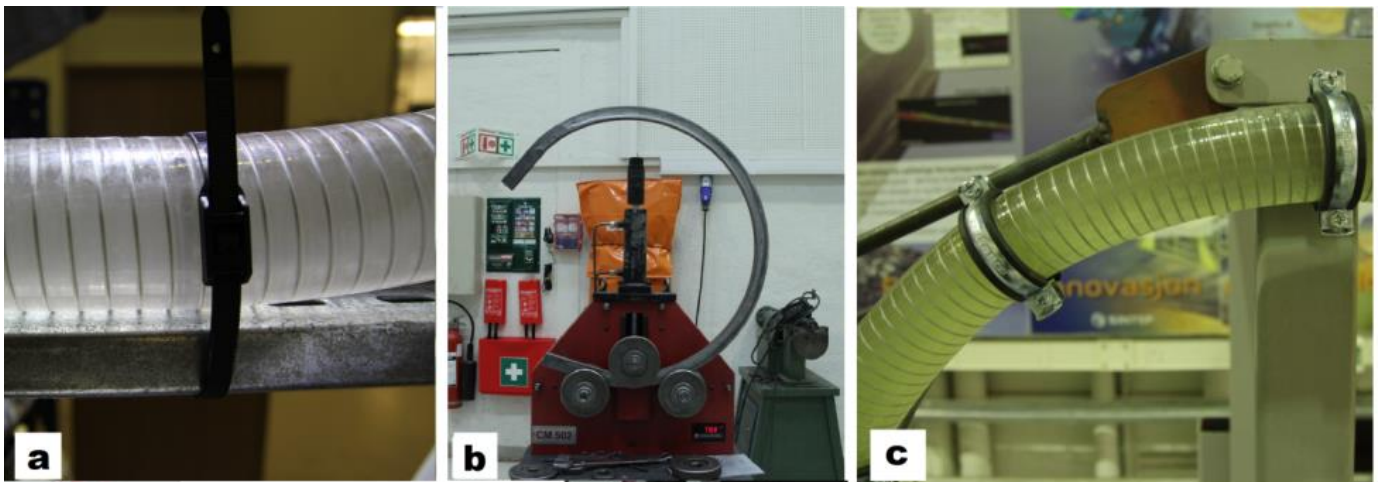


Figure 3-2: Hose support components

3.1.2 Main dimension of the rig

The initial part of the hose is connected to the S-riser fluid supplier and end part of the hose is continued till first separator. An overall view of the jumper section is shown in **Figure 3-3 a**. **Figure 3-3 b** gives schematics representation of the test rig with dimension.

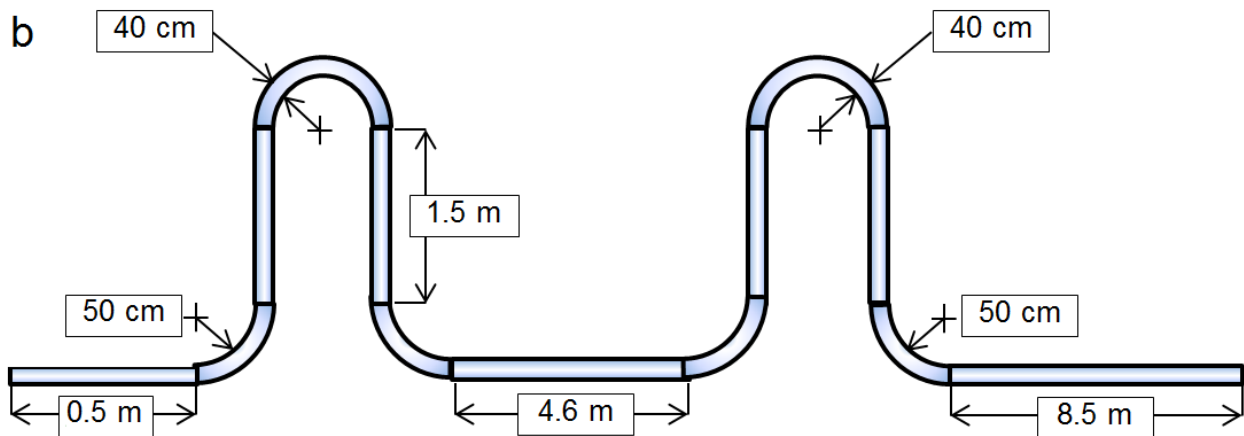
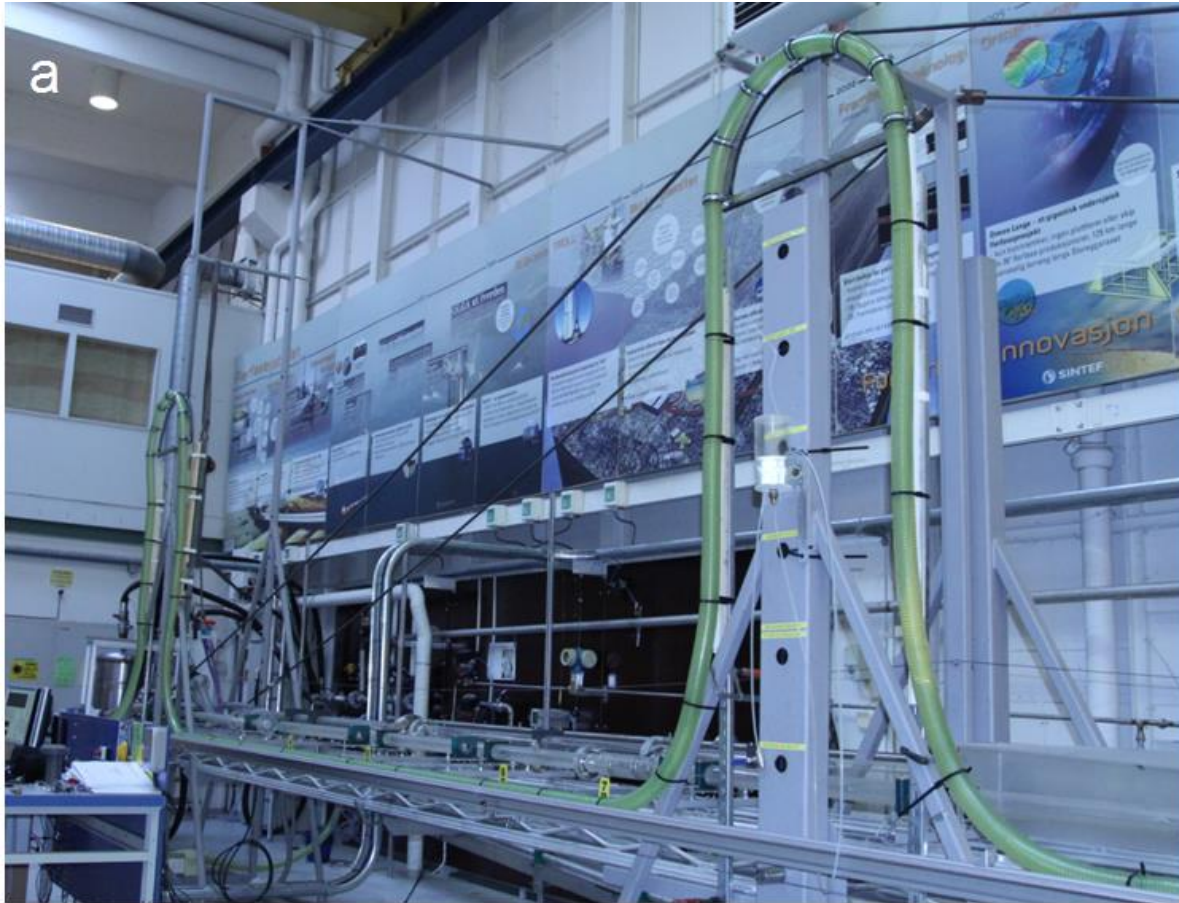


Figure 3-3: Jumper test setup – dimension

Two series conductance probe was connected to the end of the hose and the additional hose add to the probes for guiding flow into the separator. A tripod was placed in front of the probe in order to support camera for capturing. A view of additional part of the setup is given in **Figure 3-4**.

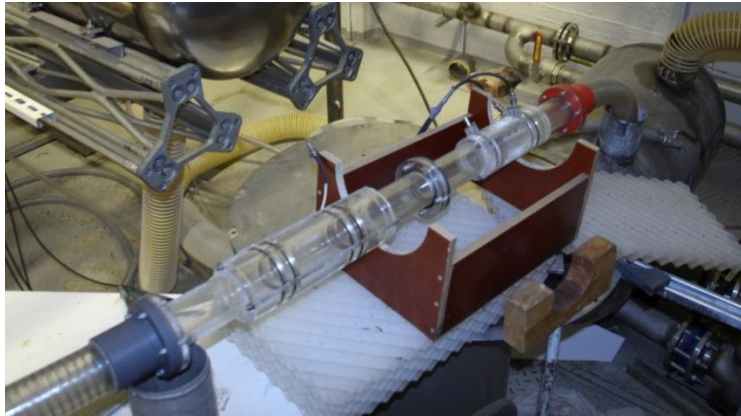


Figure 3-4: The end parts of setup (probes and additional hose)

3.2 Horizontal rig setup

Horizontal rig actually is a part of multiphase flow loop which is started after supply mixed section and ended to upstairs gas-liquid separator. This part of the loop is consisting of 60-mm and 90-mm transparent acrylic pipe. In this experiment the 60-mm has been used. Initially the loop was ready; however it required some manipulation in order to achieve the best condition for our purposes. In the follow parts the main issue will be reviewed.

3.2.1 Overview and main dimension of rig

The horizontal rig position has been changed due to required inclination of tests. Moreover some additional parts have also been attached to the rig. All flow line and pipes section which have been used in the rig for these series of test, was 60-mm inlet diameter. **Figure 3-5** is shown the overall picture of the rig with corresponded dimension.

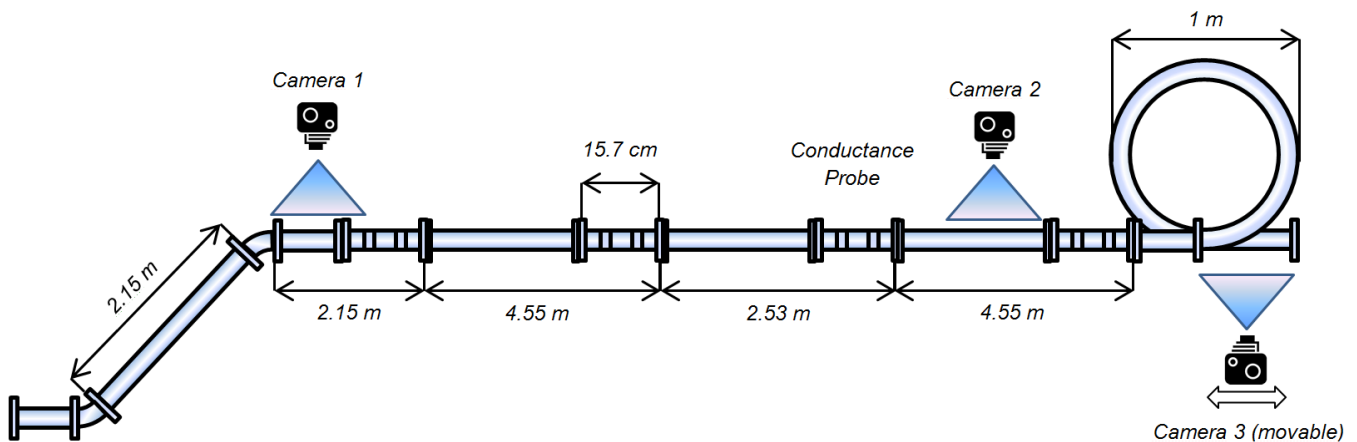


Figure 3-5: Horizontal (inclined) rig overview and dimension

3.2.2 Additional start and end section

Since series of tests are carried out in the V-shaped and also the horizontal loop was inclined, the pipe was needed starting section which has been installed as it shown in **Figure 3-6**. At the end of the pipe is also another section was required for preventing discharge of the liquid. For this part a piece of 60-mm flexible hose was utilized which is turned around itself and ended to the separator. The end section is shown in **Figure 3-6**.

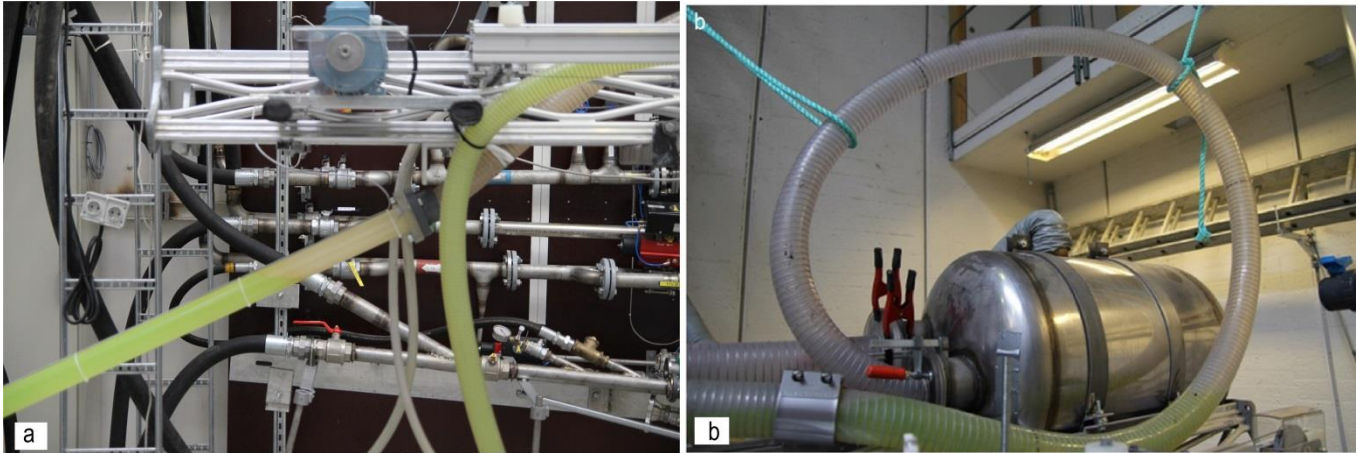


Figure 3-6: Additional start and end pipe section

3.2.3 Air Release valve

The loop sucks air from leakage point when is running and always air bubble exists in the flow lines. When the flow was stopped for establishment of initial condition, the air bubbles was merging together and a significant air bubble was accumulated at the top level of the loop. The universal standard automatic air vent valve has been implementing for discharge of undesirable accumulated air. This kind of valve was frequently used in water based heating systems [24]. For attaching this part to the pipe section; a Plexiglas joint part has been glowed to the pipe and a holes drilled through it as shown in Fig.

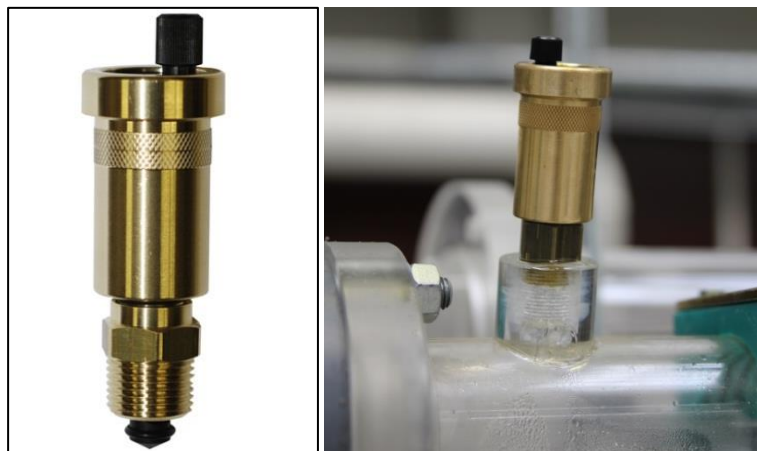


Figure 3-7: Air release valve

3.2.4 Cameras setup (stationary and movable)

Capturing of the propagation front for the viscous oil and investigation of the front shape changing has been our objective; therefore a series of cameras have been installed and utilized for this purpose. Two stationary high quality (HD) web cameras have been installed at the start and end section of the pipe flow and a movable camera which was installed in rail-carrier is capturing film. Two separate laptops were connected to the web-cam in order to store the capturing data and external storage memory card was utilized for saving movable-camera footages. The stationary cameras installed in proper distance and lightening was illuminated the back side of pipe. The movable camera was moving with one of the experiment operators with approximately the same velocity of front propagation. **Figure 3-8** is shown the rail carrier of the cameras.

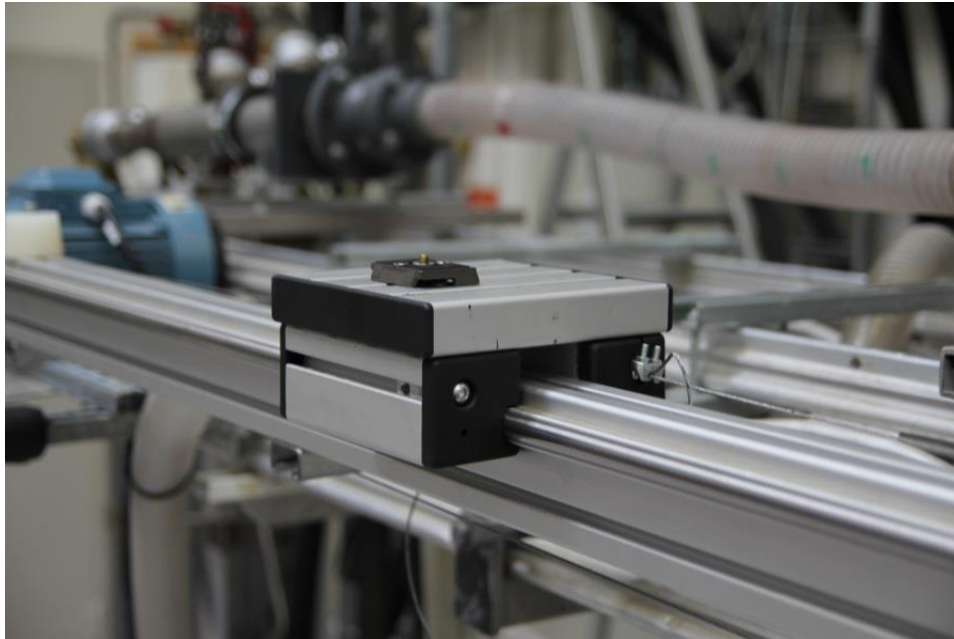


Figure 3-8: Movement camera rail system

3.2.5 Lightening system

Since one of the main objectives has been capturing of the front propagation during oil-water displacement, the lightening of the whole pipe was essential but it was challenging. Many suggestions have been evaluated. Florescent lamp was an option because of its length, but it could not utilize for this purpose due to lack of DC lightening. The accepted suggestion was using LED strips in parallel and attached in solid support. The resulting issue was non homogenous distribution of lightening because of the lamp was placed in discrete form. In order to distribute lightening in homogenous way, a semi-transparent design paper has been used such that the half of pipe was covered with it. **Figure 3-9** is shown the schematic-layered picture of lightening system.

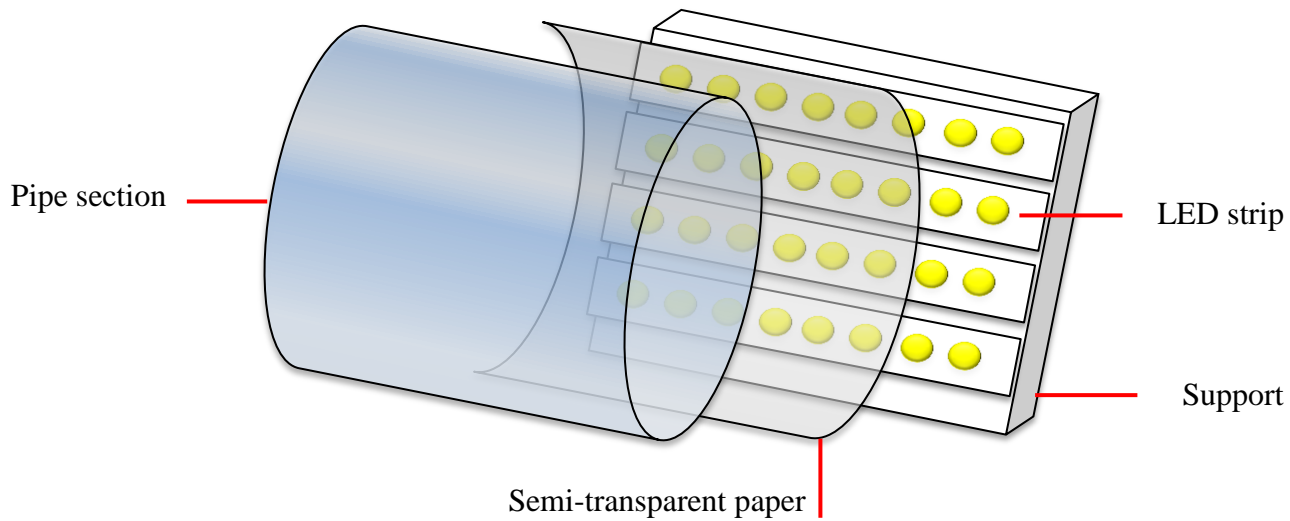


Figure 3-9: Components of lightening system

3.2.6 Anti-reflection cover

In the laboratory area, lots of light source have been exist which can be as noise for capturing. The surface of acrylic pipes are smooth such that light source can reflect. This reflection is undesirable for capturing system. Since most of the light is coming from upside of the pipe, series of opaque sheets have been placed at the top of flow line. **Figure 3-10** is shown the covering sheet system.

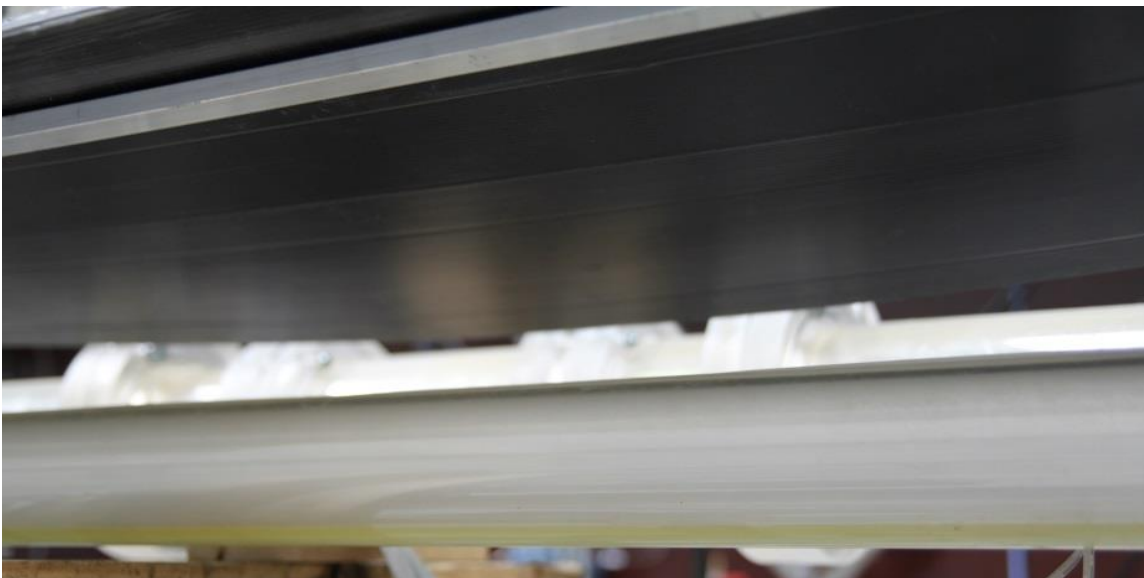


Figure 3-10: Anti-reflection cover

3.2.7 Pressure transducer and calibration procedure

In order to have pressure gradient of the flow line, the pressure transducer probe has been utilized. The pressure force in this kind of transducer is converting to the voltage which means that the each output voltage is corresponded to one absolute pressure. The logging system was store the real time pressure data in the logging storage file. **Figure 3-11** is shown a type of pressure transducer which used in this experiment.



Figure 3-11: Pressure transducer

For calibration of the pressure transducer, mini pressured-gas generator, voltage meter and pressure transducer have been applied. Pressure transducer connected to generator and the electric output connected to the voltage meter. The pressure generator produced absolute pressure up to 4.5 bars. The real time voltage appeared on the voltage meter. It means that each pressure is corresponded to voltage. **Figure 3-12** is shown one step on recording data. The record of the pressure-voltage data into excel sheet was the next step. The calibration curve is shown in **Figure 3-13**.



Figure 3-12: Calibration of pressure transducer

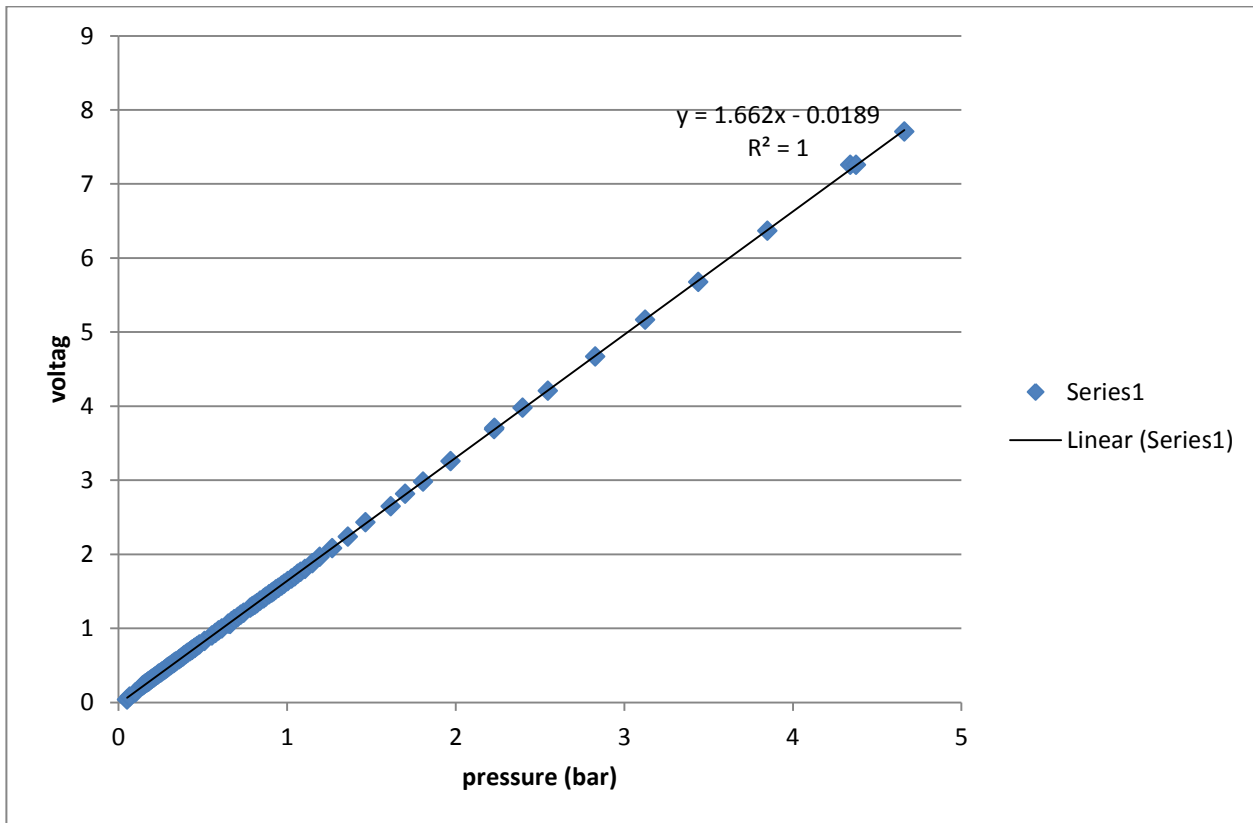


Figure 3-13: Graph of calibration of pressure transducer

3.2.8 Conductance probe and calibration procedure

Measurement of water volume fraction (water hold-up) in stratified flow regime can be measured with conductance probe such that the volume fraction of water in the pipe is proportion with the output voltage. Conductance probe has been applied for measuring the hold-up during the tests. In order to measure right amount of hold-up, the probe was calibrated. The first step for calibration is measuring the inside volume of the probe. One side of the probe was blocked with flat flange and then the probe was being completely filled with water. The volume of water was known by using an accurate measuring glass. The next steps were the logging probe with 16 known volumes of the water which increase gradually. At each step the probe filling with desired volume of water and both side of the probe got blocked. Then it placed horizontally, checked with spirit level and logging was started for about 30 second. **Figure 3-14** show the probe calibration in one of middle steps. Corresponding chart give the results of calibration. The calibration constant is calculated by linearization of the points of measurements (see **Figure 3-15**). In addition the scaling factor (0.61) needed due to conductivity difference between tap water which was used for calibration and water with fluorescent additive which runs in loop. This number is obtaining by **Equation 3-1**:

$$\text{Scaling factor} = \frac{V_{100\% \text{ filling with tap water}}}{V_{100\% \text{ filling with fluorescent water}}} \quad \text{Equation 3-1}$$

The calibration constant was implemented for all hold-up measurements since this calibration constant approximated the same for all voltage channels.



Figure 3-14: Calibration of the probe

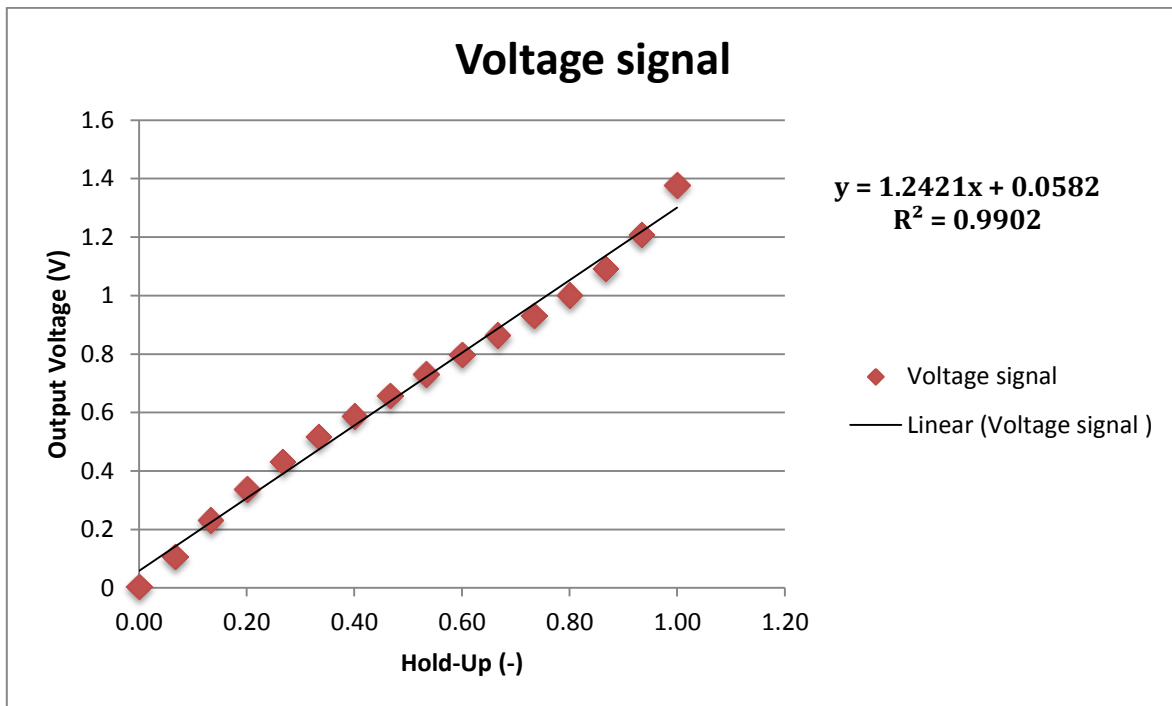


Figure 3-15: Calibration curve

3.3 Oil-water front experiment at horizontal and inclined pipe

The series of tests have been conducted for understanding of propagation of oil and water column during the restart process. The test has been run in the horizontal loop rig. NEXBASE® 3080 was the using oil. The experiment can be divided into four main series. Two series carried out in horizontal (0 degree) inclination and the others two series have been conducted in inclined (2.8 degree). In the following part each test series will be described. Capturing and logging were been the common thing in all experiment series. Two stationary cameras, a moving camera, conductance ring probes and pressure transducer were including for measurement and logging system. The detail steps of procedure can be found in Appendix B. Oil has been changed to the NEXBASE at the big separator before running the test.

3.3.1 Oil bubble flushing with water at inclined test section

The first test series of front propagation have been conducted at horizontal loop with +2.8 degree inclination. Each test has been run after initial condition establishment. In order to set the initial condition, first the whole loop was filled with water. The next step was to open the valve for making an oil bubble bulk in the heist point of the loop. After reaching to the desired volume of oil bubble, the oil valve was closed. 19 tests have been run after establishment of initial condition with various water flow rate. The logging and capturing was binging before run the water into the loop.

3.3.2 Fully filled oil pipe flushing with water at inclined test section

The inclination was the same for these test series. The oil has been filled in additional first part and in whole of the flow lines. In order to set the initial condition, small amount of water has been injecting to the loop such that the level of water has reached at the middle of additional first pipe section. The desired flow rate adjusted at the parallel test loop. The desired flow rate then has been switch to the horizontal loop. Logging the probes and also three capturing module have started just before run the water into the loop.

3.3.3 Fully filled oil pipe flushing with water at horizontal test section

In this experiment, the additional inclined pipe section still available. The loop was first filled with oil. The additional first section was half-filled with water and the initial condition was established. The test was run with 17 different water flow rates which have been already adjusted in parallel loop. The test was beginning when the flow was switched to the horizontal loop. Logging and capturing was started just before water flow into the loop. **Figure 3-16-a** is shown test setup.

3.3.4 Fully filled water pipe flushing with oil at horizontal test section

The pipe which was filled fully with water has been flushing out with two different oil flow rate. First the initial condition was established. The initial condition was the pipe filled with water and a bubble of oil was stand at the beginning of pipe section. **Figure 3-16-b** is shown the initial condition in this test series. The next step for run the experiment was adjusting the desired flow rate in the jumper loop. When the desired flow rate has been reached, the valves were switching flow to the horizontal loop. Capturing and logging was started just before water flow into the loop.

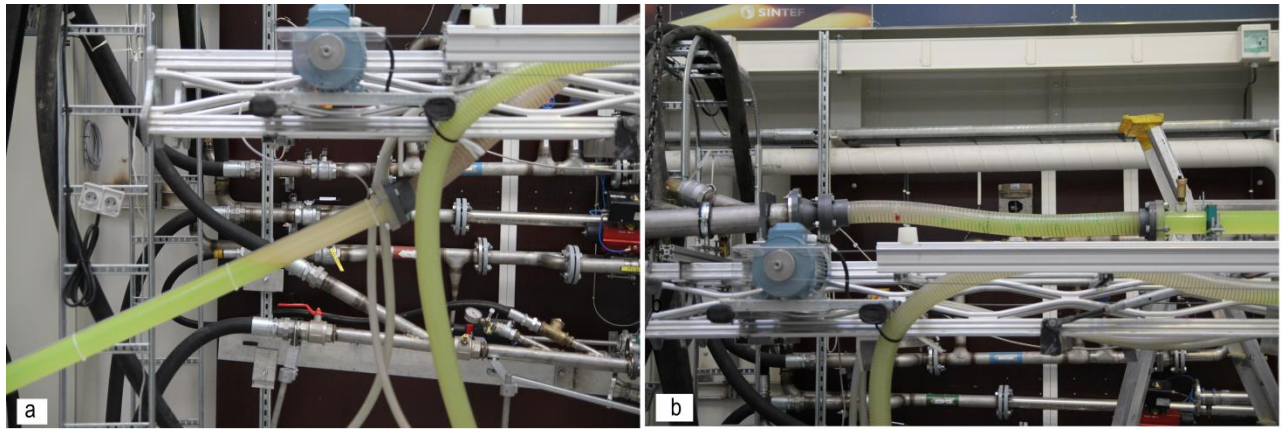


Figure 3-16: Initial condition for horizontal pipe flushing

3.4 Oil-water flushing test in M-shaped jumper test

These series of the experiments have been conducted for describing the front shape of the oil-water when water is flushing the residual oil in the jumper. Exxon D80 was the using oil in the tests. This experiment was valuable due to run the flow into the special jumper setup. 16 tests were conducted with different water flow rate. In each experiment first the initial condition was established which means the pipe filling with oil until the middle of the first vertical section and before horizontal curvature (point A) and rest of the jumper was filled with water. **Figure 3-17** gives the schematic and real picture of initial condition for the experiment.

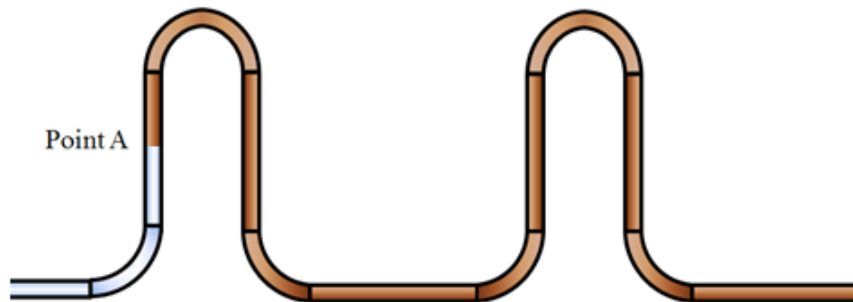


Figure 3-17: Initial condition in jumper

After establishment of the initial condition the desired flow rate adjust in the horizontal pipe. The test started by switching the oil flow from the horizontal pipe to the jumper. The flow rate was being set in reasonable value (such as 1.20 Kg/s or 1.60 Kg/s) but when the flow was switched to the jumper, the flow rate was started to reduce due to gravity and friction of jumper flow line. Therefore measured flow rate was different but it still had reasonable increasing steps. All new flow rates was measured and put to the corresponded results. The logging was started a few second before flow run to the jumper. The camera captured flow through the probe frequently and sequences of picture at high capturing continues mode was collected. The detailed explanation of the experiment procedure can be found at the Appendix C. The result of these series of tests is presented in following sections.

4 Results of Experiments and Discussion

This chapter presents the results of all series of experimental activities which was described in chapter 3. The discussions of the results are expressed besides.

4.1 Oil bubble flushing with water at inclined test section

19 tests have been conducted in order to studying the flushing phenomena. Some experiments have been repeated twice for compensating of technical issues; therefore the final tests are given in following matrix **Table 4-1**. The experiments put in low to high water flow rate.

Table 4-1: Oil bubble flushing test matrix

tag #	experiment tag	U _{sw} (m/s)	Flow rate m ³ /s	length of oil bubble (cm)
1	flushing_24apri_exp12_1441	0.1716	0.0004852	132
2	flushing_24apri_exp10_1356	0.179	0.0005061	183.5
3	flushing_24apri_exp13_1501	0.19496	0.0005512	141.5
4	flushing_23apri_exp6_1532	0.2022	0.0005717	68.9
5	flushing_24apri_exp11_1420	0.20385	0.0005764	90.5
6	flushing_24apri_exp14_1519	0.28579	0.0008081	87
7	flushing_24apri_exp15_1529	0.28962	0.0008189	129.5
8	flushing_24apri_exp16_1546	0.38119	0.0010778	133
9	flushing_23apri_exp5_1519	0.3972	0.0011231	230
10	flushing_24apri_exp9_1212	0.42112	0.0011907	189.5
11	flushing_24apri_exp8_1139	0.43732	0.0012365	82.5
12	flushing_24apri_exp7_1116	0.4734	0.0013385	69
13	flushing_23apri_exp4_1455	0.526	0.0014872	231

Based on observation from pictures of the movable camera, qualitatively description of these series of tests has been reported in **Table 4-2**. Two parts, one in the beginning section and another at the end section have been discussed. The relative sharpness of the front, smoothness of interface and water hold up fraction and special issues have been reviewed. The pictures will be shown at the Appendix D.

Table 4-2: Observation results of oil bubble

#	U_{sw} (m/s)	Beginning section of pipe	End section of pipe
1	0.1716	The interface is wavy. The water holdup gradually increases from near 0.5 to 1 in front. Some dispersed oil droplets in water are observed in the front.	The interface gets sharper. The average water hold up is more here than beginning section.
2	0.179	The interface is very smooth and not wavy. The water holdup gradually increases from approximately 0.5 to 1 in the front.	The whole bubble is take to part and the remaining front of bubble get very sharp
3	0.19496	The water holdup increase from less than 0.5 to 1. The interface is approximately is smooth. Some oil droplets are in the interface.	The front gets sharper. The bulk of dispersed oil in water accumulated in front.
4	0.2022	The smooth interface with hold up from 0.5 to 1 in the front.	The interface get wavy and the front get sharper.
5	0.20385	The interface is wavy. Some oil droplets have accumulated in the front.	The front is full of oil dispersed droplets.
6	0.28579	The bubble has been separated in two parts. The interface is wavy and with some oil bubbles in the interface.	The water hold up is dominated. The residual oil part is thin, wavy and with dispersed oil droplets in water.
7	0.28962	The oil bauble part is wavy and water holdup is dominated.	The front is full of oil dispersed droplets. The interface is wavy
8	0.38119	The water holdup is more than 0.5 and interface is smooth and the front is sharp.	The interface is wavy and oil droplet is accumulated in the front.
9	0.3972	The front is approximately vertical. The water hold up is more than 0.5 and the interface is smooth.	Some relatively big oil droplets accumulate in the front. The interface is not wavy and the water hold up is more than half.
10	0.42112	The water hold up less than 0.5 and the interface is smooth and gradually increase to more than 0.5. The initial part of the front is sharp and the front is approximately vertical.	The front is very sharp and some oil bubble is separated. The interface is wavy and with dispersed oil droplets.
11	0.43732	The level of oil bubble is not change. The water hold up is higher than 0.5. The interface is very smooth.	The interface is wavy and oil droplet is observed in the interface. Some part of bubble is separated to some parts.
12	0.4734	The interface is wavy. Water hold up is more than 0.5 and increase gradually.	The bubble is divided into the separate part. The oil droplets can be observed in bubble parts.
13	0.526	The interface is ramped. Few oil droplets are observed in the interface. The interface is smooth.	The bubble is separated. The water hold up is more than 0.5. The interface is wavy with some oil droplets.

Figure 4-1 is shown that the typical holdup vs. time for three different conductance probe in different position along the horizontal pipe. All 13 graphs can be found in Appendix E. From water holdup measurement graph which is measured with conductance probes the further result can be summarized:

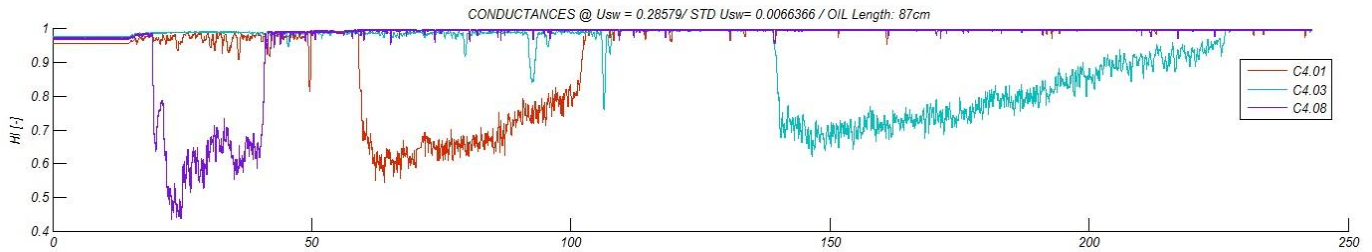


Figure 4-1: Typical conductance probes logging graph

- 1- The bubble is remaining in the pipe in superficial water velocity less than 0.179 m/s.
- 2- The time of bubble passing decreased in each probes by increasing the injection water superficial velocity.
- 3- The time of bubble passing increased along the pipe. In the constant velocity and based on hold up measurement graph, the bubble is get longer in the end of pipe.
- 4- The front part of the bubble at relatively high velocity has flat tip, which means that in the front edge of bubble we have sudden drop in water holdup in high velocity.

4.2 Fully filled oil pipe flushing with water at inclined test section

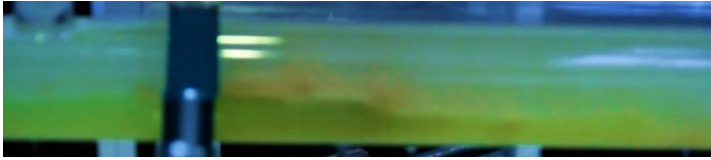
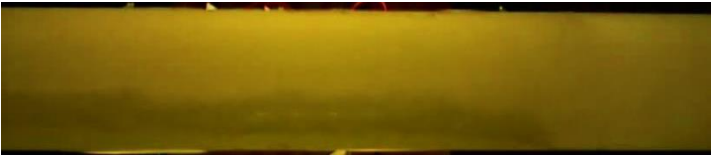
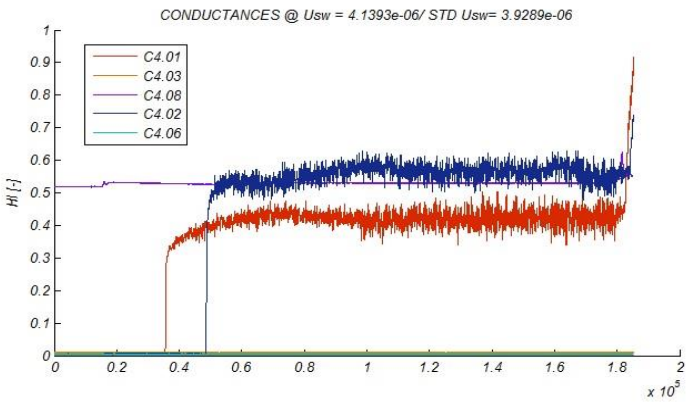


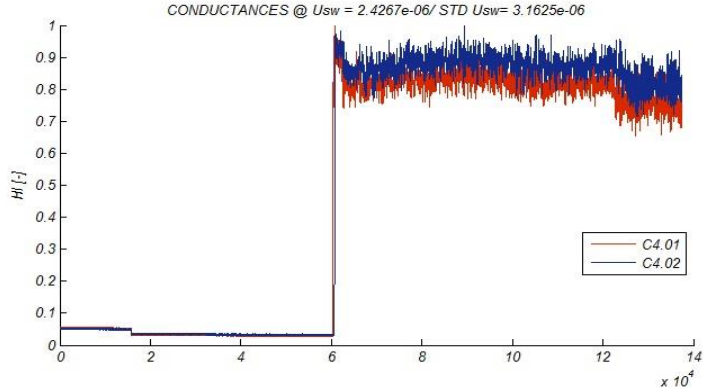
Two different tests have been conducted in order to studying the flushing phenomena. The final tests are given in following matrix **Table 4-3**. The experiments put in low to high water flow rate.

Table 4-3: Inclined pipe oil flushing by water test matrix

tag #	experiment tag	U_{sw} (m/s)	Flow rate m^3/s
1	flushing_29apri_exp20_0926	0.102	0.000200277
2	flushing_29apri_exp21_1011	0.0202	3.96626E-05

The capturing pictures of beginning and end section and in addition the water holdup measurement graphs are presented in **Table 4-4**.

Table 4-4: Inclined pipe oil flushing by water graph and pictures

U_{sw} (m/s)	section	Figures
0.102	Beginning	
	End	
	Water holdup	 <p>CONDUCTANCES @ $U_{sw} = 4.1393e-06$ / STD $U_{sw} = 3.9289e-06$</p>
0.0202	End	
	Beginning	
	Water holdup	 <p>CONDUCTANCES @ $U_{sw} = 2.4267e-06$ / STD $U_{sw} = 3.1625e-06$</p>

From start and end section and water holdup measurement graph which is measured with conductance probes show that:

- 1- At the beginning and at the end section of the pipe the front part is sharp.
- 2- In both flow rates the oil volume fraction at the beginning of the pipe is more than the end of the pipe.
- 3- The flushing efficiency (removing the oil) has been increased by increasing of the water injection flow rate.

The average water holdup at the start and end section of the two flow rates is shown in **Table 4-5**.

Table 4-5: Average water holdup

U_{sw} (m/s)	Water holdup (-)	
	Start section	End section
0.102	0.421	0.563
0.0202	0.790	0.849

4.3 Fully filled oil pipe flushing with water at horizontal test section

17 tests have been conducted in order to studying the flushing phenomena. Some experiments have been repeated twice for compensating of technical issues; therefore the final 7 tests are given in following matrix **Table 4-6**. The experiments put in low to high water flow rate.

Table 4-6: Horizontal pipe oil flushing by water test matrix

tag #	Experiment tag	U_{sw} (m/s)	Flow rate m^3/s
1	flushing_25mar_exp14_1543	0.05	9.81748E-05
2	flushing_25mar_exp13_1525	0.1	0.00019635
3	flushing_25mar_exp10_1448	0.15	0.000294524
4	flushing_25mar_exp9_1437	0.19	0.000373064
5	flushing_25mar_exp7_1400	0.28	0.000549779
6	flushing_25mar_exp2_1255	0.38	0.000746128
7	flushing_25mar_exp5_1341	0.49	0.000962113

The water holdup measurement graphs are presented in **Table 4-7**.

Table 4-7: Conductance probe measurement graph

Us _w (m/s)	Figures
0.05	
0.1	
0.15	
0.19	
0.28	
0.38	
0.49	

From the holdup measurement graph which is measured with conductance probes the further results show that:

- 1-The critical water superficial velocity for flushing all oil from the pipe is 0.384 m/s because all oil flushed out from pipe after this water flow rate.
- 2- The front part of propagation of water is getting more flat in higher velocity.
- 3- The oil volume fraction in lower velocity is higher.

4.4 Fully filled water pipe flushing with oil at horizontal test section

Two different tests have been conducted for investigation of water flushing phenomena with oil. The final tests matrix is given in **Table 4-8**. The experiments put in low to high water oil superficial velocity.

Table 4-8: Horizontal pipe water flushing by oil test matrix



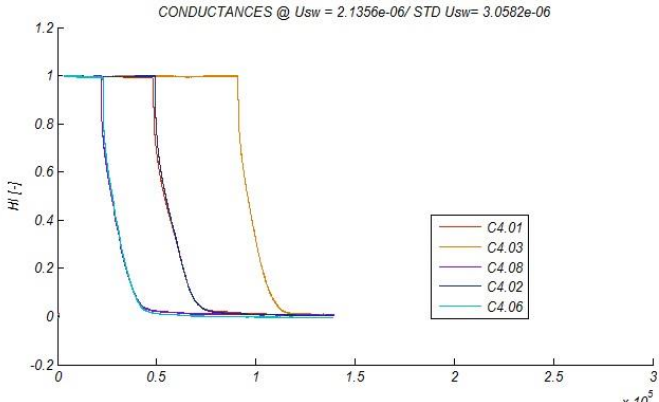


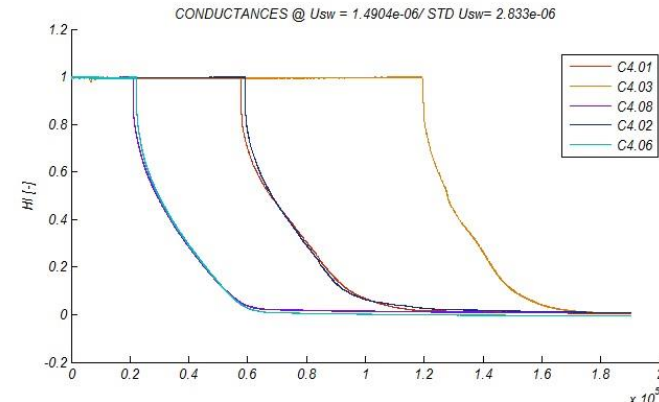
Tag #	Experiment tag	U_{s_o}	Flow rate m^3/s
1	flushing_29apri_exp26_1644	0.053	0.000104065
2	flushing_29apri_exp25_1626	0.078	0.000153153

The capturing pictures of beginning and end section and in addition the water holdup measurement graph are presented in **Table 4-9**.

From start and end section and water holdup measurement graph which is measured with conductance probes the further result show that:

- 1-Both in beginning and end section of the pipe the front part is sharp and gradually water holdup decreases.
- 2- The behavior of the propagation front along the pipe is the approximately the same.
- 3- Both flow rates of oil have flushed out and removed the whole of water from the pipe.

Table 4-9: Graph and pictures of horizontal pipe water flushing by oil

U_{sw} (m/s)	section	Figures
0.053	Beginning	
	End	
	Water holdup	 <p>CONDUCTANCES @ $U_{sw} = 2.1356e-06$ / STD $U_{sw} = 3.0582e-06$</p>
0.078	End	
	Beginning	
	Water holdup	 <p>CONDUCTANCES @ $U_{sw} = 1.4904e-06$ / STD $U_{sw} = 2.833e-06$</p>

4.5 Oil-water flushing test in M-shaped jumper test

Concerning qualitative explanation of flushing experiment, as commented in test description, various water flow rates run through the jumper such that in each step oil flow rate was increased gradually. Another aim of this part was finding the water injection velocity for totally removing of oil from jumper. After sufficient time the flow in jumper became steady-state and transient phenomena has not observed anymore. Considerable point of the jumper setup was captured during the steady-state condition. The explanations is divided and identified by the oil flow rate in following **Table 4-10**. The whole oil was removed along jumper after water injection superficial velocity higher than **0.38** m/s as can be seen in **Table 4-10**.

Table 4-10: Observation of tests in the jumper

U_{s_w} [m/s]	Comment
0.01	The middle jumper section slowly filling, water droplets in oil continuum in both down comers, risers filled with water.
0.02	As previous flow rate, more water droplets in down comer, and more droplets in elbow and droplet with relatively small size can be observed.
0.04	As before, more water droplets in down comer, more droplets in elbow, droplet size 0.2 - 1cm (more small droplets) , right after increasing the velocity, some oil was transported through the horizontal section, hard to say which phase the continuous is, looks like phase inversion in pipe sometimes
0.08	In this flow rate oil droplets in water continuum (visible from droplet movement), in the lower elbow we found an accumulation of many small oil droplets, oil droplet size smaller as water droplets, 0.3 - 0.7 cm
0.11	By increasing flow rate the oil is transported through horizontal section as thin film or droplets on top part, as before, many small oil droplets 3mm in lower elbow, larger droplets 1cm in upper part
0.16	Down comer almost pure water, only a few oil droplets, oil accumulation in top section left, and still many small droplets in lower elbow
0.2	As before, even less droplets in down comer, only some droplets in top section, still many droplets in lower elbow
0.25	Top section and down comer pure water, only some residual droplets can be observed in lower elbow.
0.32	The lower elbow is almost empty.
0.38	The jumper is totally empty.

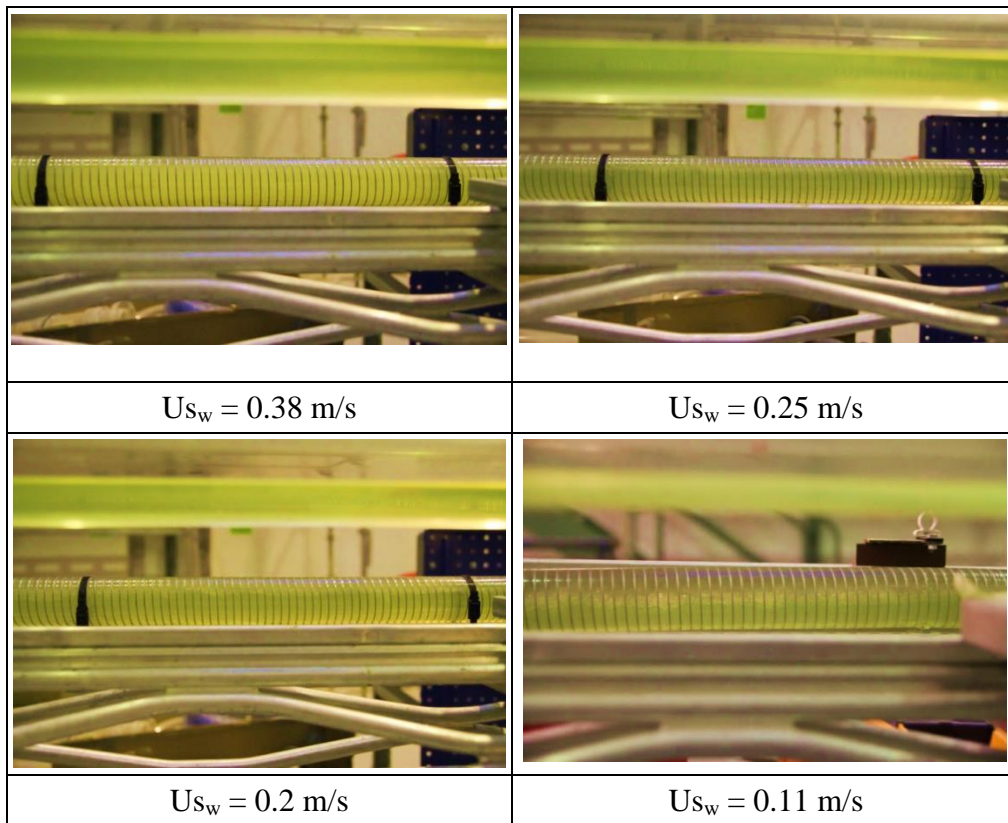


Figure 4-2: Middle section in the jumper at 4 different velocities

Some experiments were executed in order to study the oil-water front. The results were given in **Table 5-2** and **Figure 5-5** (both experimental and simulation are presented in the same graph). The water removing time for each individual test equals to the period between the first oil droplet is coming ($\alpha_o \neq 0$) and last water droplet goes out ($\alpha_w = 0$). The trend of data is indicated that the required time for displacement of the water with oil decreased by increasing the water mass flow rate. Typical water hold up graph which was measuring with conductance probe is shown in the **Figure 4-3**. The water remove time is indicated with the red line. All trend graphs could be found in Appendix F.

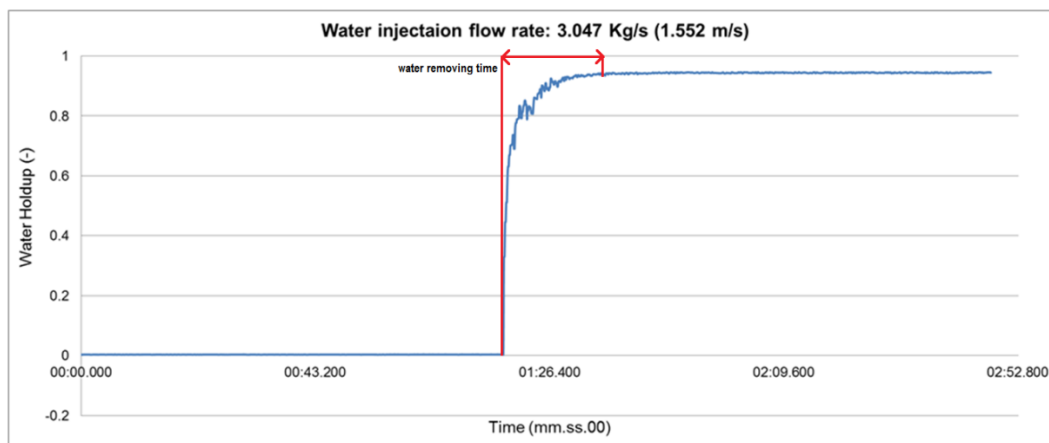


Figure 4-3: Typical water hold up at the end of pipe measurement

5 Simulation of experimental cases, results and discussion

In this chapter the simulation of the individual test runs are presented. In section 5.1, the case construction is stepwise explained with implementing the M-shaped jumper geometry, fluid properties, numerical setting and boundary condition. Section 5.2 deals with the results and comparison of water-oil front estimation cases.

5.1 Construction of the case

The initial steps for simulation process is establishment of a case with particular items such as: fluid properties, numerical setting, initial and boundary condition, flow path geometry and meshing setup.

5.1.1 Flow path geometry and meshing

The jumper geometry was simulated in LedaFlow® based on the measurements. 81 points were defined (81 parts) in order to represent jumper geometry. Curvatures was drawn by put the corresponding points in each 10° and use trigonometry relations to calculate Cartesian coordinate positions (**Figure 5-1**). Geometry specification will be found in Appendix H. The uniform algorithm method was utilized for meshing the geometry. 150 mesh cells have been chose for a reasonable simulation time, simulation stability and simulation accuracy. crated and the length of each cell was about 0.16 m. **Figure 5-2** gives an overview of the geometry that has been established in simulation.

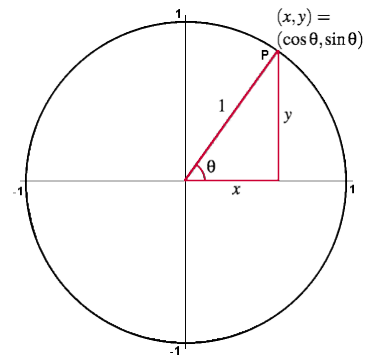


Figure 5-1: X-Y Position of curve

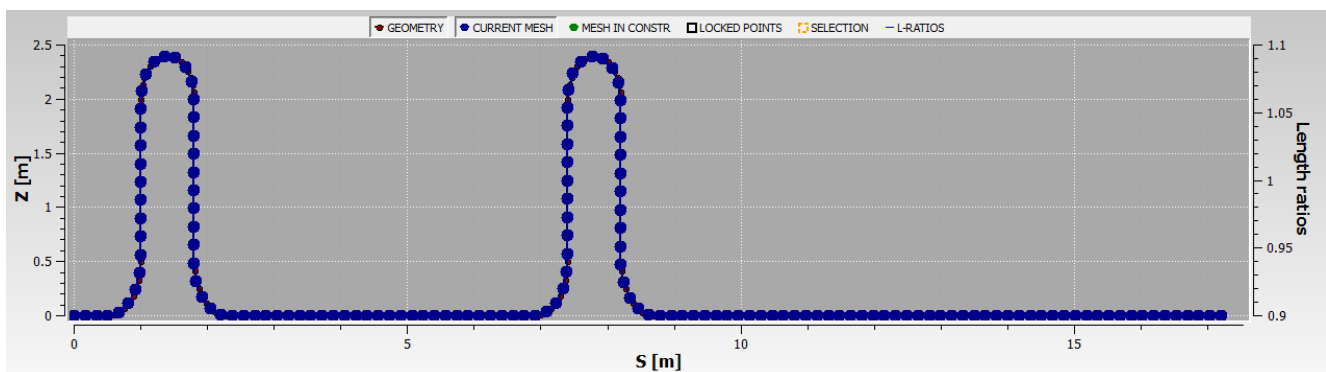


Figure 5-2: Pipe geometry in simulator

5.1.2 Fluid properties

All fluid properties were written in PVT file. Heat transfer and temperature change was not care in the simulation due to experiment condition. The oil-water flow was also assumed as an incompressible flow. Therefore 2×2 table (two pressure points and two temperature points) was enough for each property. The interpolation and extrapolation option in the simulator were set to operational mode for calculation of the fluid properties. Heat transfer and temperature related properties such as enthalpy or entropy were being filled with dummy number. Oil and water densities, viscosities, surface tension and oil-water interfacial tension have been written in PVT file. The properties values could be found in **Table 3-1**.

5.1.3 Boundary Condition

The type of the inlet nod was defined as inlet mass flow. In each simulation case, the flow rate was changed to desired number. The water volume fraction was established to 1 while oil and gas fraction was set to 0. The outlet nod type was selected to pressure type and it has been set to atmospheric pressure.

5.1.4 Initial Condition

Since Leda Flow 1D has not any option to establish initial condition manually, a dummy case about 10 second with fully water was run (water cut 100%) and the restart file was crated. The same simulation was run but this time with 100% oil. By studying the restart test file, the phase fraction and phase velocity format for each mesh cell was found. Then the restart file was converted to the initial condition file by manipulating of the restart file. Velocity and volume fraction for each mesh (150 points) have been replaced one by one to get initial set condition. The time of restart file was also set to 0. **Figure 5-3 a** shows that in time = 0, phases volume fractions, and phases velocities (both phases equal zero) is given in **Figure 5-3 b**.

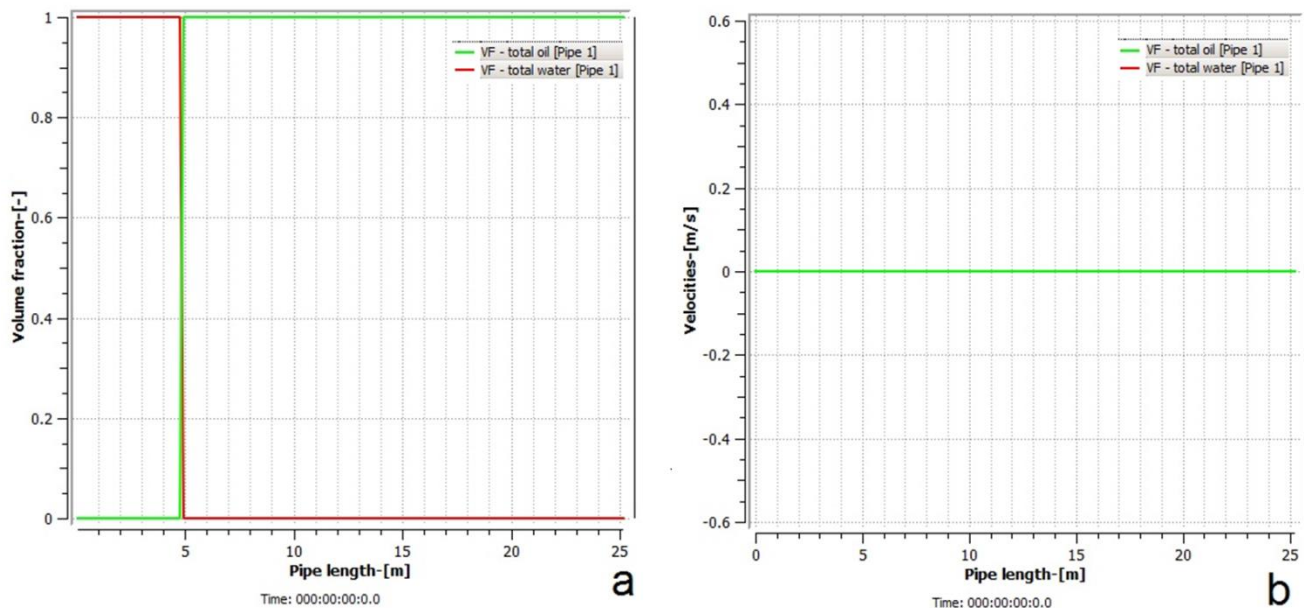


Figure 5-3: Initial condition in simulation

5.1.5 Numerical setting

The numerical setting specification such as simulation time, sample time, time step and CFL was adjusted in different number from case to case. This happens because of the phase velocity diversity in different cases. The range of the numerical setting is given in **Table 5-1**. These properties were selected based on typical values and try and error. For instance many time steps have been tried for reasonable simulation time and accuracy. The typical CFL suggested in LedaFlow® guidance. [22]

Table 5-1: Numerical setting values

Numerical properties	Minimum value	Maximum value
Simulation time	100	5000
Time step	0.005	1
Sample time	0.1	3
CFL*	0.7	0.8

* CFL: The number ensures a time step is sufficiently low in relation to the grid cell length and the phase velocities

5.2 Oil-water front simulation results

Figure 5-4 gives a typical trend data for volume phase fraction at the end of the jumper. Corresponded data was used in order to compare the experimental data regarding oil-water front shape estimation.

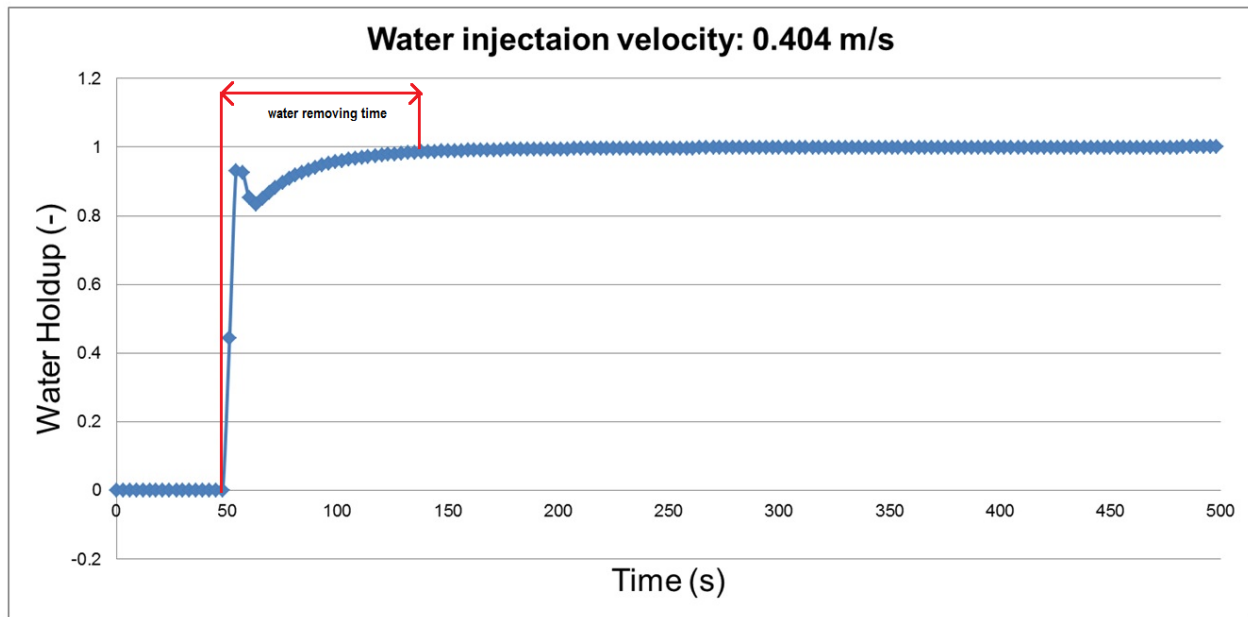


Figure 5-4: Typical phase volume fraction at the end of pipe by simulation

7 simulations were run in order to study the oil-water front as the same values in the experiment. The results were given in **Table 5-2** and **Figure 5-5**. The time for each simulation equals to the period between the first oil droplet is coming ($\alpha_o \neq 0$) and last water droplet goes out ($\alpha_w = 0$). Here, it is clear

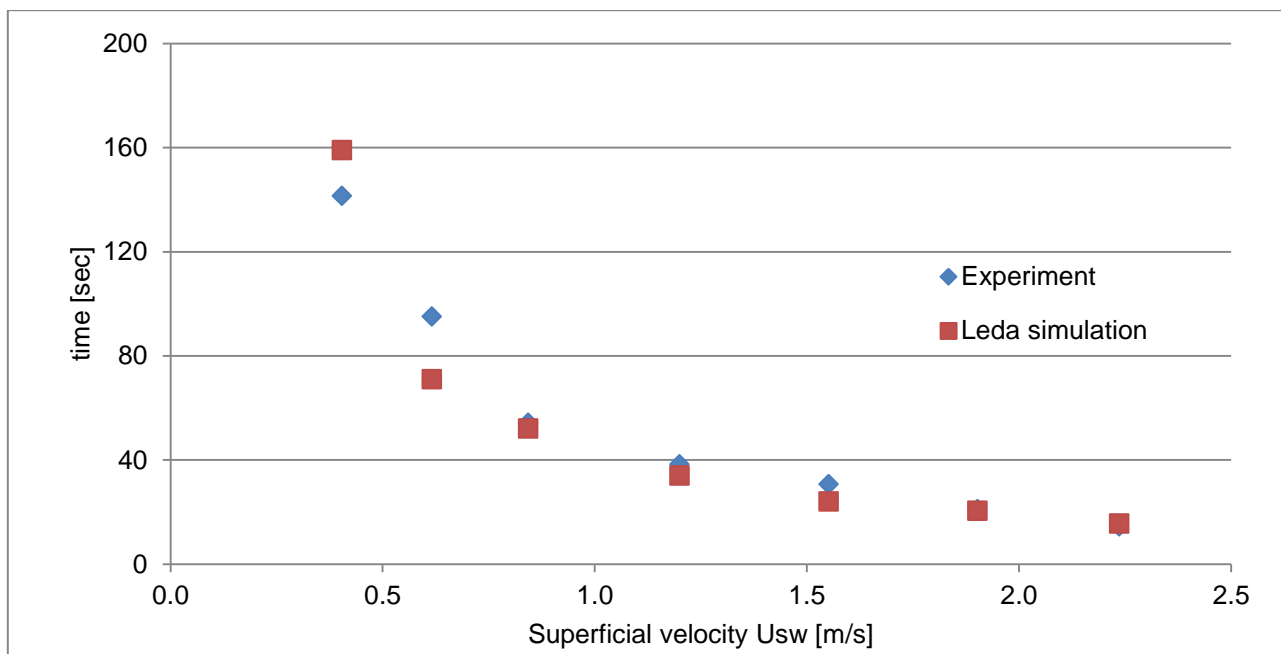
that the required time for displacement of the water with oil increases by increasing the oil mass flow rate. All trend graphs could be found in Appendix I.

In comparison with experiment, the overall trend for both experiment and simulation is the same. However, dramatically difference is observed in relative low flow rate.

Table 5-2: Removing water time, represents interface oil-water front

Test #	U_{sw} [m/s]	Water Remove Time[s](simulation)	Water Remove Time[s](experiment)
1	0.404	141.459	159.000
2	0.616	95.063	71.000
3	0.843	54.282	52.000
4	1.200	38.266	34.000
5	1.552	30.641	24.000
6	1.903	21.097	20.400
7	2.236	14.360	15.540

Figure 5-5: Removing water time, represents interface oil-water front



6 Conclusions and recommendation for further works

The defined tasks in the project description were tracked and the looked-for results obtained. Some tasks were done in order to prepare the setup of tests. Oil-water flushing experiment and corresponded simulations have been conducted.

The preparation of setup for both horizontal/inclined rig and small scale M-shaped jumper has been designed and done in NTNU multiphase laboratory. In addition the simulation case was constructed and the main conclusions of each effort are listed in follow.

The experiment of oil bubble flushing with water at inclined test section indicated that:

- At the beginning part of pipe, the interface of front part was approximately smooth and without oil droplets nearly at all different flow rates.
- At the end part of pipe, the interface of front part was wavy and with oil droplets nearly at all different flow rates.
- The water hold up reduces along the pipe and therefore the front shape gets sharper at the end of pipe.

The test of fully filled oil pipe flushing with water at inclined test section showed that:

- Both in beginning and end section of the pipe the front part was sharp and no propagation difference observed along the pipe.
- Water hold up at the beginning of the pipe was less than the end of the pipe in both flow rates.
- The flushing efficiency (removing the oil) has been increased by increasing the water injection flow rate.

The experiment of fully filled oil pipe flushing with water at horizontal test section indicated that:

- The front part of propagation of water was getting more flat in higher water flow rates.
- The oil volume fraction in lower velocity was higher.
- The critical water superficial velocity for flushing all oil from the pipe was around 0.384 m/s.

The tests of fully filled water pipe flushing with oil at horizontal test section showed that:

- The behavior of the propagation front shape was the approximately the same along the pipe.
- Both in beginning and end section of the pipe the front part was sharp.

The M-shaped jumper flushing experiment results mainly indicated:

- No oil remained in the jumper if a certain superficial velocity was exceeded, for our test this critical velocity was around 0.38 m/s.
- The required time for displacement of the water with oil decreased by increasing the water mass flow rate.

The M-shaped jumper flushing test runs cases have been simulated at multiphase flow simulator, LedaFlow. The initial condition, fluid properties and geometry of tests have been set similarly to simulator. The simulation results showed:

- The time of removing residual water in setup decreased by increasing the oil mass flow rate.

The comparison between results of simulation and experiment indicated that:

- At relative low oil mass flow rates, the simulation and experiment have given different results but in same trend.
- Difference between test and simulation value was higher at relatively low velocity based on value comparison.

Recommendations for further works:

Here some suggestions are listed below:

- Running the series of experiment in other geometries with various inclinations.
- Conduction of these experiments can be tested at the other pipe diameters like 50 mm or 90 mm.
- Conducting the same experiment can be evaluated for various oil viscosity and different temperature.
- Preparation of setup without optical obstacles (pipe supports) in order to capture continuously.
- Providing the setup with more stationary cameras with a managing control system.
- Using CFD programming model to evaluate prediction of particular flow model.
- Capturing through the pipe with high speed camera especially at higher flow rate.

7 References

1. Danielson, T., et al. *Simulation of Slug Flow in Oil and Gas Pipelines Using a New Transient Simulator*. in *Offshore Technology Conference*. 2012.
2. Guðmundsson, J.S., *FLOW ASSURANCE SOLIDS*, 2011.
3. Guo, D.B., et al., *Chapter 15 - Flow Assurance*, in *Offshore Pipelines*. 2005, Gulf Professional Publishing: Burlington. p. 169-214.
4. Larsen, R., *Natural Gas Hydrates - the "Mother of all Flow Assurance Challenges"*, 2009.
5. ASPO. *Association for the Study of the Peak Oil*. 2012; Available from: www.asponews.org.
6. Zhang, H.-Q., D. Vuong, and C. Sarica, *Modeling High-Viscosity Oil/Water Cocurrent Flows in Horizontal and Vertical Pipes*. *SPE Journal*, 2012. **17**(1): p. 243-250.
7. Guevara, E., J. Gonzalez, and G. Ninez. [8] *4 Highly Viscous Oil Transportation Methods in the Venezuelan Oil Industry*. in *15th World Petroleum Congress*. 1997.
8. Makinde, F., et al., *PREDICTION OF CRUDE OIL VISCOSITY USING FEED-FORWARD BACK-PROPAGATION NEURAL NETWORK (FFBPNN)*. *Petroleum & Coal*, 2012. **54**(2): p. 120-131.
9. Rennels, D.C. and H.M. Hudson, *Fundamentals*. *Pipe Flow: A Practical and Comprehensive Guide*: p. 3-12.
10. Abedini, R., A. Abedini, and N.E. Yakhfrouzan, *A New Correlation for Prediction of Undersaturated Crude Oil Viscosity*. *Petroleum & Coal*, 2010. **52**(1): p. 50-55.
11. Hemmingsen, P.V., et al., *Emulsions of heavy crude oils. I: Influence of viscosity, temperature, and dilution*. *Journal of dispersion science and technology*, 2005. **26**(5): p. 615-627.
12. Kumara, W.A.S., *An Experimental Study of Oil-Water Flow in Pipes*, 2010, Norwegian University of Science and Technology Telemark University College Faculty of Technology: Porsgrunn.
13. Nydal, O.J., *Stratified flow, Lecture Material*, 2012.
14. Trallero, J., C. Sarica, and J. Brill, *A study of oil-water flow patterns in horizontal pipes*. *Oil Production & Facilities*, 1997. **12**(3): p. 165-172.
15. Abduvayt, P., et al. *Analysis of Oil-Water Flow Tests in Horizontal, Hilly-Terrain, and Vertical Pipes*. in *SPE Annual Technical Conference and Exhibition*. 2004.
16. Arirachakaran, S., et al. *An analysis of oil/water flow phenomena in horizontal pipes*. in *SPE Production Operations Symposium*. 1989.
17. Nydal, O.J., *Mixture Flow, Lecture Material*, 2012.
18. Bratland, O., *Pipe Flow 2 Multi-phase Flow Assurance*. Ove Bratland, 2010.
19. Bai, Y. and Q. Bai, *Chapter 21 - Subsea Connections and Jumpers*, in *Subsea Engineering Handbook*, B. Yong and B. Qiang, Editors. 2010, Gulf Professional Publishing: Boston. p. 663-701.
20. Worren, H.I.K., *Displacement of liquid in pipe flow: Two-dimensional simulations*, 2012, Norwegian University of Science and Technology: Trondheim. p. 81.
21. Danielson, T., et al. *LEDA: the next multiphase flow performance simulator*. in *BHR Group Multiphase Production Technology Conference*. 2005.
22. Technologies, K.O.G., *LedaFlow® Flow Assurance for 21 st Century Oil & Gas Production Training Course Handouts*. 2011.
23. Chupin, G., *Experimental Studies of Gas-Liquid and Gas-Liquid-Liquid Pipe Flow at Low Liquid Loading*, in *Energy and Process Technology 2003*, Norwegian University of Science and Technology: Trondheim.
24. Jennings, B.H. and S.R. Lewis, *Air conditioning and refrigeration*. 1944: International textbook company.

Appendices

Appendix A

The summary of risk assessment of horizontal loop are presented here.



Risk Assessment Report

Multiphase Flow Loop- Horizontal loop Experiments

Prosjekttittel	Multiphase Flow Loop- horizontal-pipe Experiments
Prosjektleder	Ole Jørgen Nydal
Enhet	NTNU
HMS-koordinator	Erik Langørgen
Linjeleder	Olav Bolland
Plassering	Energy and Process Technology Laboratory
Romnummer	Multiphase Flow Laboratory
Riggansvarlig	Ole Jørgen Nydal
Risikovurdering utført av	Erik Langørgen, Seid Ehsan Marashi

• **ATTACHMENT G PROCEDURE FOR RUNNING EXPERIMENTS**

Experiment, name, number: Multiphase Flow Loop- Horizontal-Loop Experiments	Date/ Sign
Project Leader: Ole Jørgen Nydal	
Experiment Leader: Mariana Diaz	
Operator, Duties:	

Conditions for the experiment:	Completed
Experiments should be run in normal working hours, 08:00-16:00 during winter time and 08.00-15.00 during summer time. Experiments outside normal working hours shall be approved.	
One person must always be present while running experiments, and should be approved as an experimental leader.	
An early warning is given according to the lab rules, and accepted by authorized personnel.	
Be sure that everyone taking part of the experiment is wearing the necessary protecting equipment and is aware of the shut down procedure and escape routes.	
Preparations	Carried out
Post the "Experiment in progress" sign.	
Clear the area around the loop. There should be no open containers with oil/water or oil/water on the floor.	
Check pressure regulator for air system -35	
See that there is free access to the air valve, HV 1001 from air tank in basement. Emergency shutdown valve for the system	
First start the air loop by slowly opening HV1001. HV4003 and HV10012 shall be kept open. Other valves (HV10006, HV10007, HV10008, HV10009, HV10010 have to be opened according to the procedure for small or large air flow) Control valves can be opened slowly using labview. The other valves are used of small flowrates are desired. At the end of the S-riser there is a control valve, but this has been disconnected and is always open to avoid pressure buildup.	
Then start the water loop by opening HV2003. Next you open the valve in front and behind the pump you choose. Make sure HV2002, HV3014, HV11001, HV11003 and HV11012 are always closed during operation. HV11002, HV11011 shall be open.	
Then switch the pump on and control its point of operation by adjusting its frequency and adjusting the control valves. If the frequency is too low (less than 10 Hz) you may not get any flow.	
During the experiment	
<i>Control of leakage in the set-up</i>	
Control air pressure, and that's enough for not filling tank V-35 with water	
End of experiment	
Turn off the liquid pumps and close the control valves.	

	Purge the loop with air.	
	Then slowly close of the air control valve.	
	<p>Valves should be back at the initial position or as needed for the next experiment. The final valves positions have to be in accordance with the use of the loop:</p> <ul style="list-style-type: none"> • Centrifugal pumpes or positive displacement pumps. • Riser or horizontal rig. 	
	Remove all obstructions/barriers/signs around the experiment.	
	Tidy up and return all tools and equipment.	

Appendix B

Explanation of details regarding procedure for the horizontal flushing experiment is listed in **Table 0-1**. The valves which are mentioned at the procedure are referred to **Figure 0-1** which gives a schematic of the jumper and horizontal loop.

Table 0-1: Experimental procedure, flushing water in horizontal

Step	Action	Comment
1	Close all valves (CV1-3 and V1-6)	
2	Open V1	
3	Open CV1 gradually and simultaneously run the oil pump up	To reach the desired flow rate we use jumper
4	Set the flow rate to desired flow rate (set by U_{s0})	
5	Make a logging file and start the logging (for hold up)	
6	Start capturing in multiple cameras system	
7	At a moment change flow from jumper to horizontal by closing V1 and opening V6	First close V6 and then open V1
8	Move the third camera along the pipe with flow propagation	To have front shape
9	Wait to separate two phases	
10	Stop the experiment when no water goes out	Run the horizontal to reach high oil flow rate

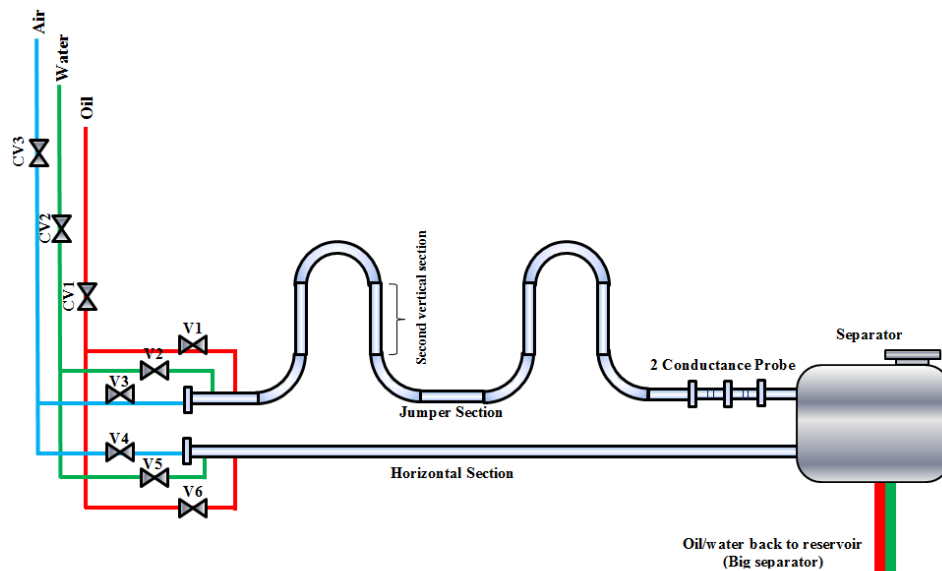


Figure 0-1: Test schematic configuration

Appendix C




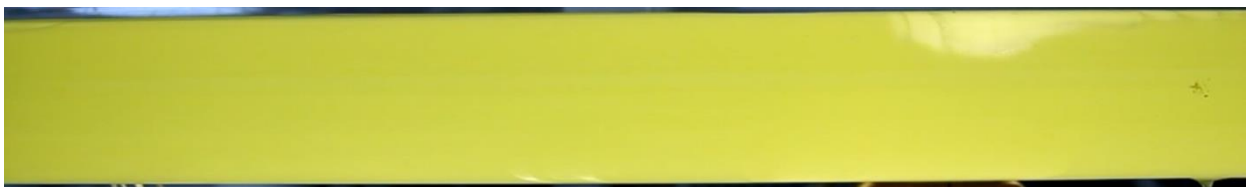


Explanation of details regarding procedure for the jumper flushing experiment is listed in **Table 0-2**. The valves which are mentioned at the procedure are referred to **Figure 0-1** which gives a schematic of the jumper and horizontal loop.

Table 0-2: Experimental procedure, flushing in jumper








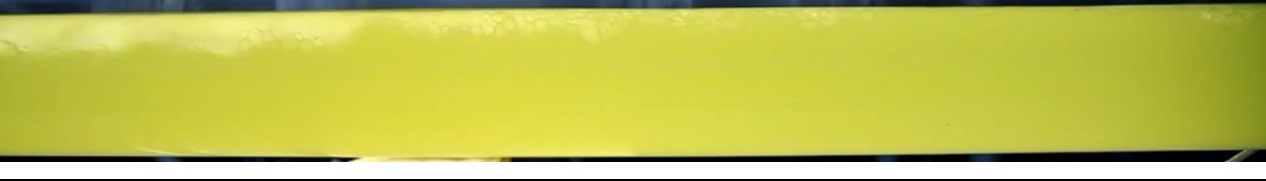
Step	Action	Comment
1	Close all valves (CV1-3 and V1-6)	
2	Open V4	
3	Open CV2 gradually and simultaneously run the water pump up	To reach the desired flow rate we use horizontal
4	Set the flow rate to desired flow rate (set by U_{s_w})	
5	Make a logging file and start the logging (for hold up)	
6	At a moment change flow from horizontal to jumper by closing V4 and opening V3	First close V4 and then open V3
7	Take a pictures at the middle pipe	To have front shape
8	Wait to separate two phase	
9	Stop the experiment when no oil goes out	Run the horizontal to reach high water flow rate





Appendix D

All figures with different mass flow rate are represented in this section. All data are relevant to oil-water front simulation.

U_{sw} (m/s)	section	Figures
0.171	Beginning	
	End	
0.179	Beginning	
	End	
0.194	Beginning	
	End	

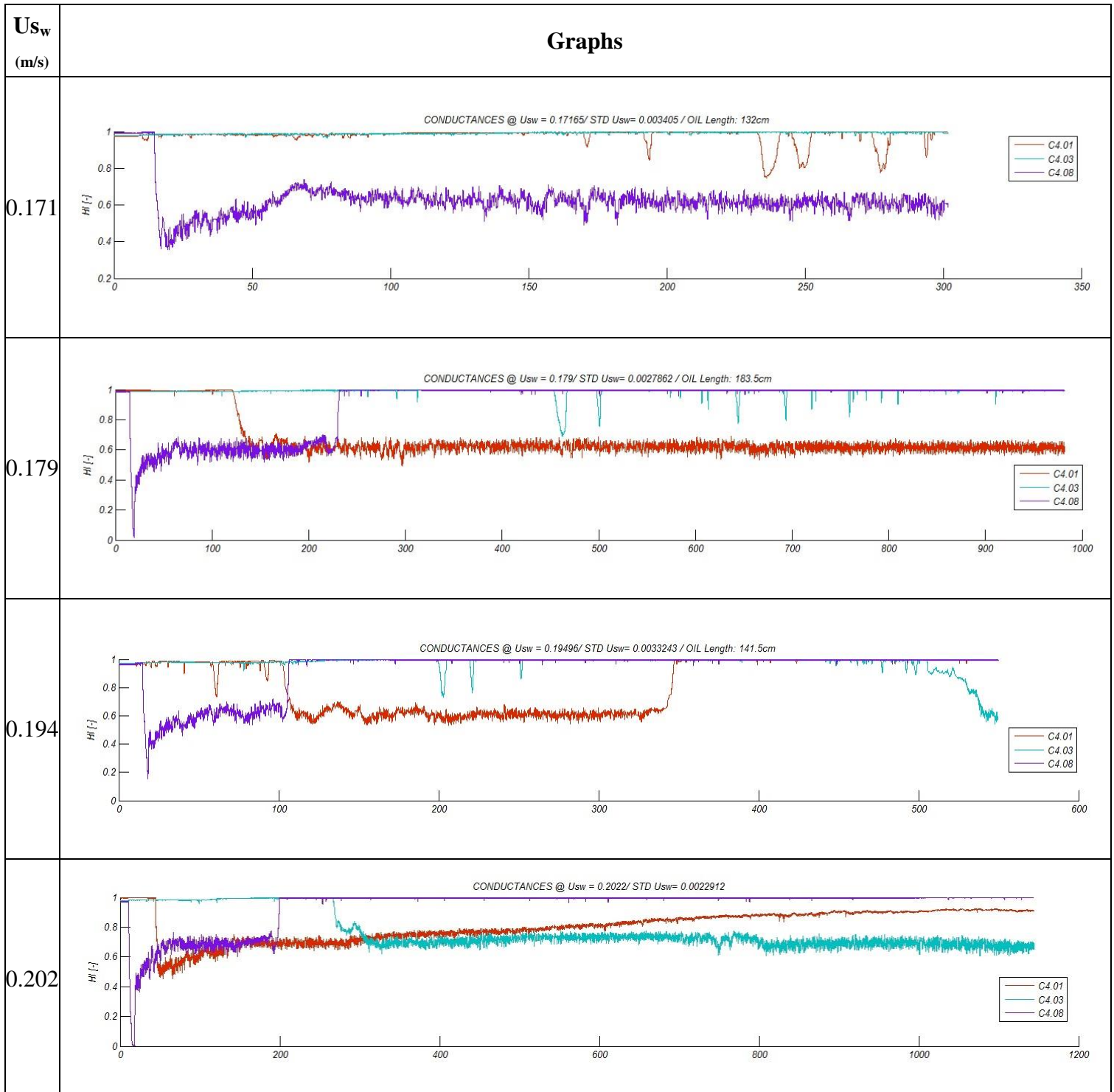
U_{sw} (m/s)	section	Figures
0.202	Beginning	
	End	
0.203	Beginning	
	End	
0.285	Beginning	
	End	
0.289	Beginning	
	End	

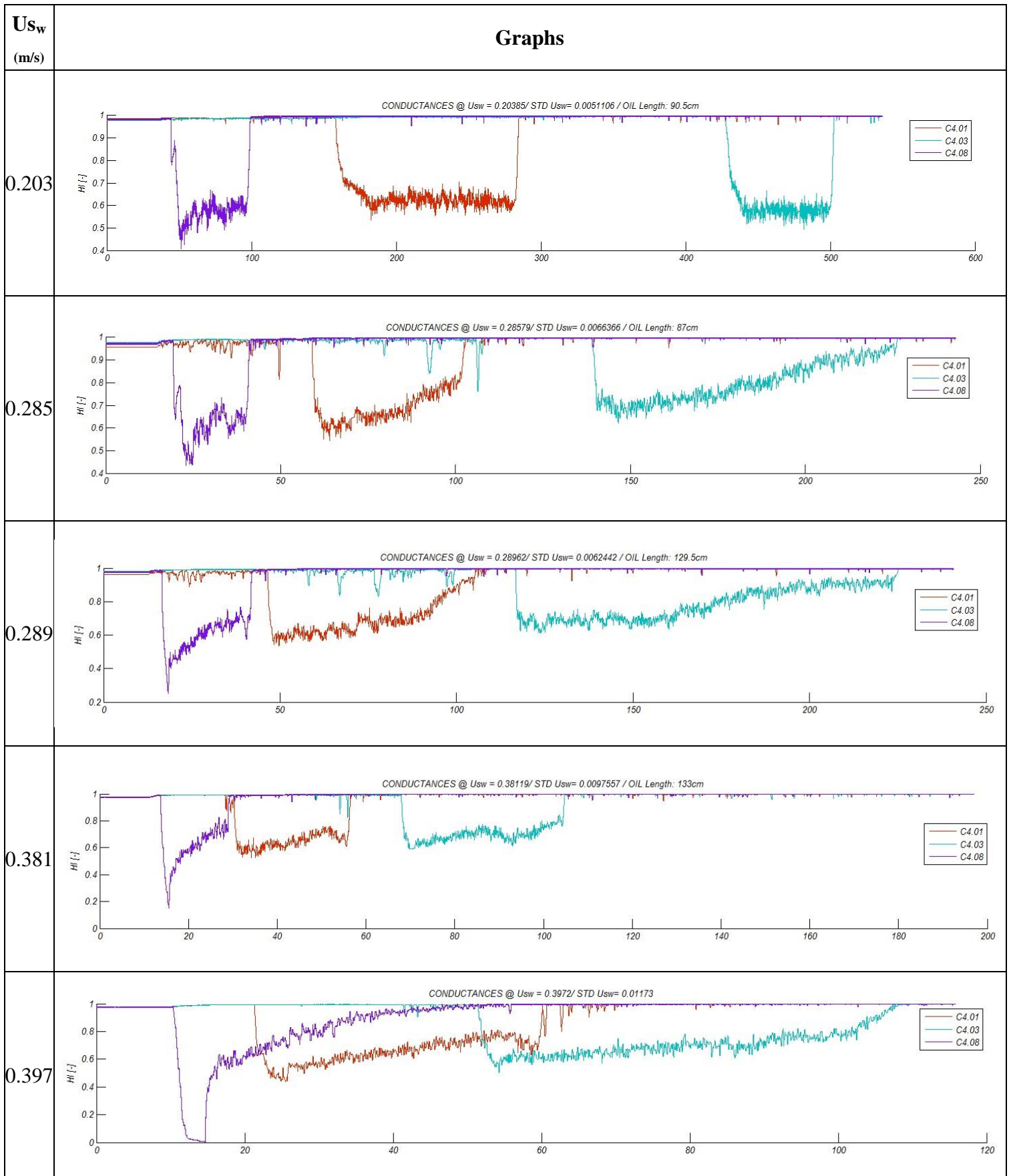
U_{sw} (m/s)	section	Figures
0.381	Beginning	
	End	
0.397	Beginning	
	End	
0.421	Beginning	
	End	
0.437	Beginning	
	End	

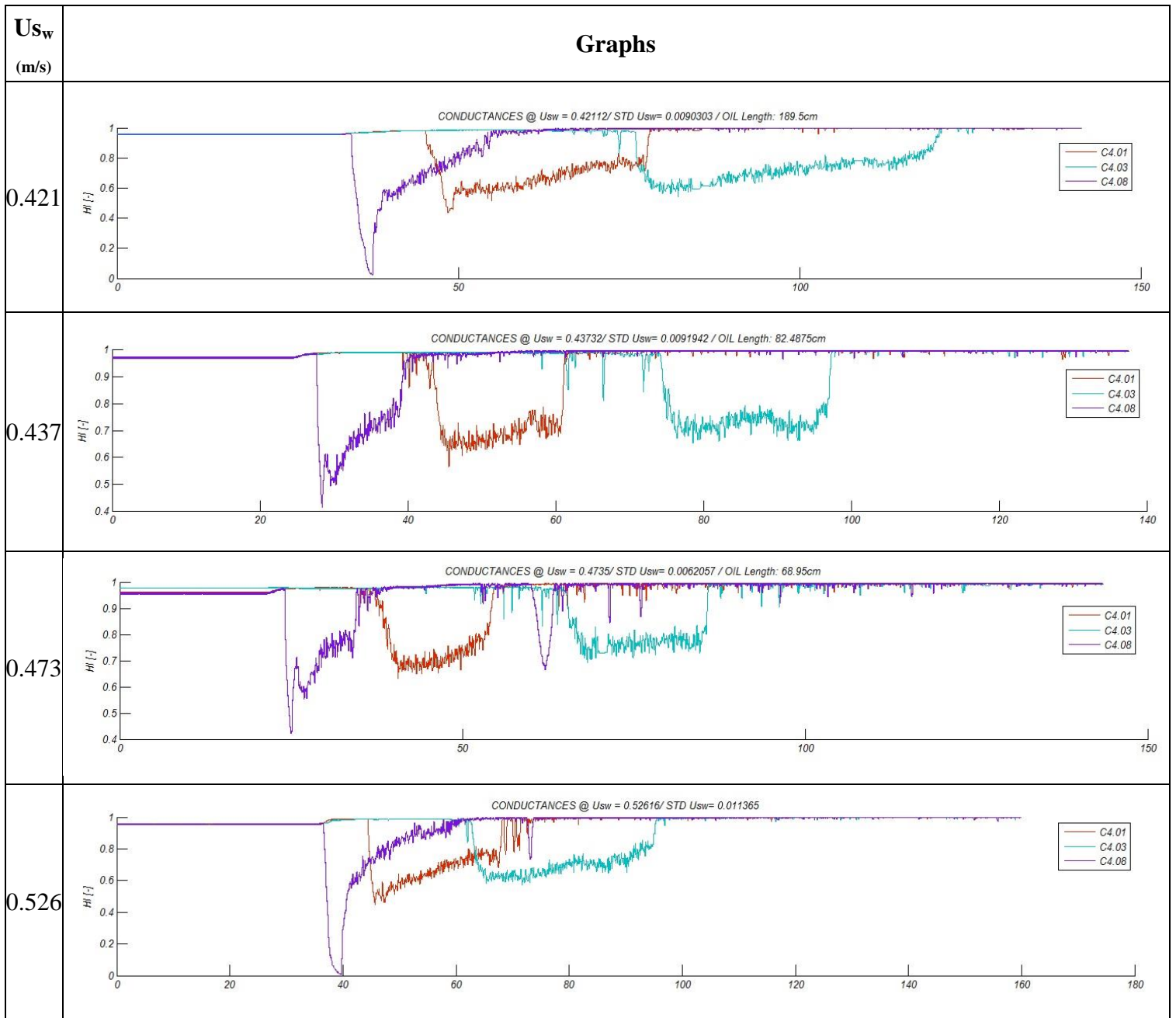
U_{sw} (m/s)	section	Figures
0.473	Beginning	
	End	
0.526	Beginning	
	End	

Appendix E

All water hold up (-) vs. time(s) graphs with different mass flow rate are represented in this section. All data are relevant to oil-water front experiments.

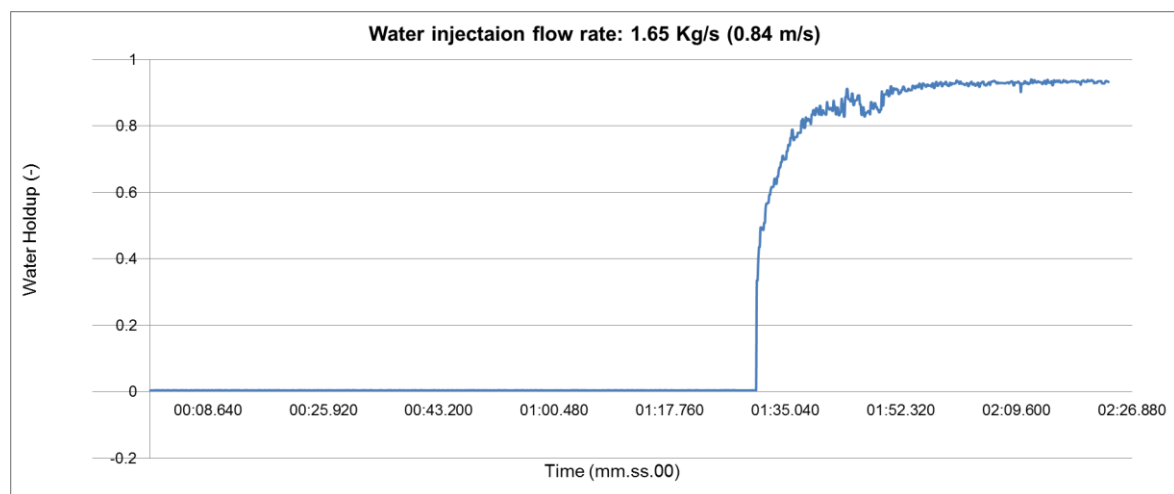
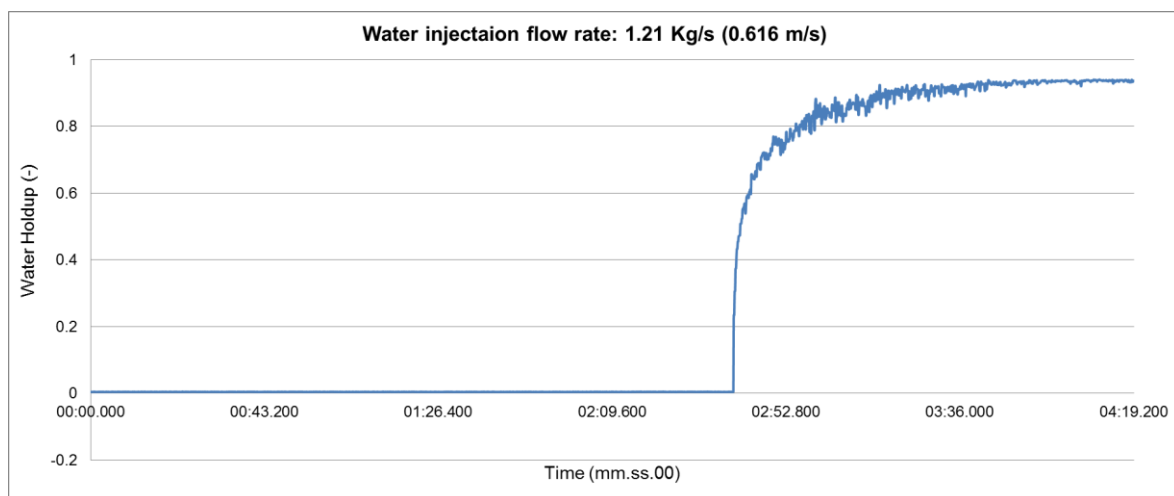
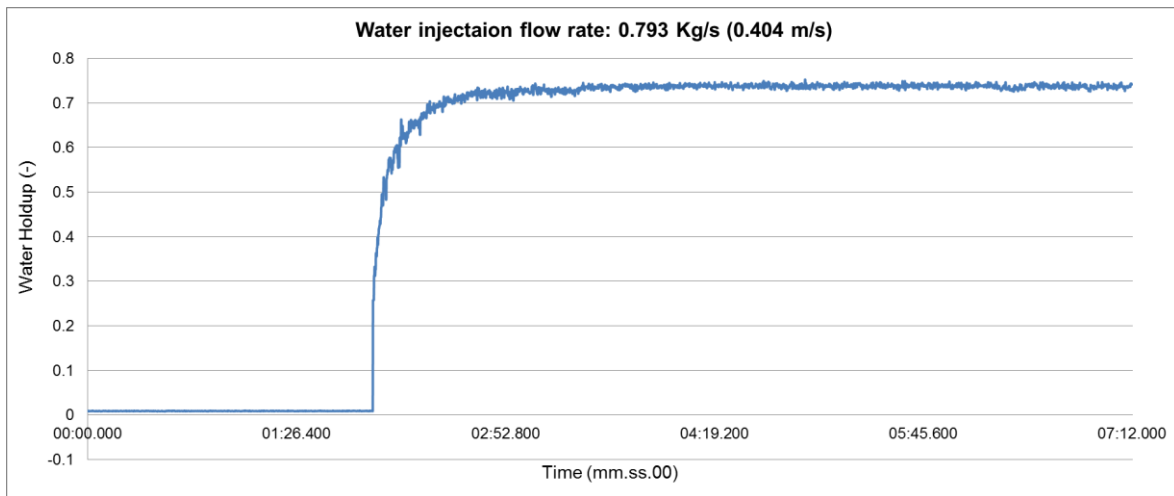


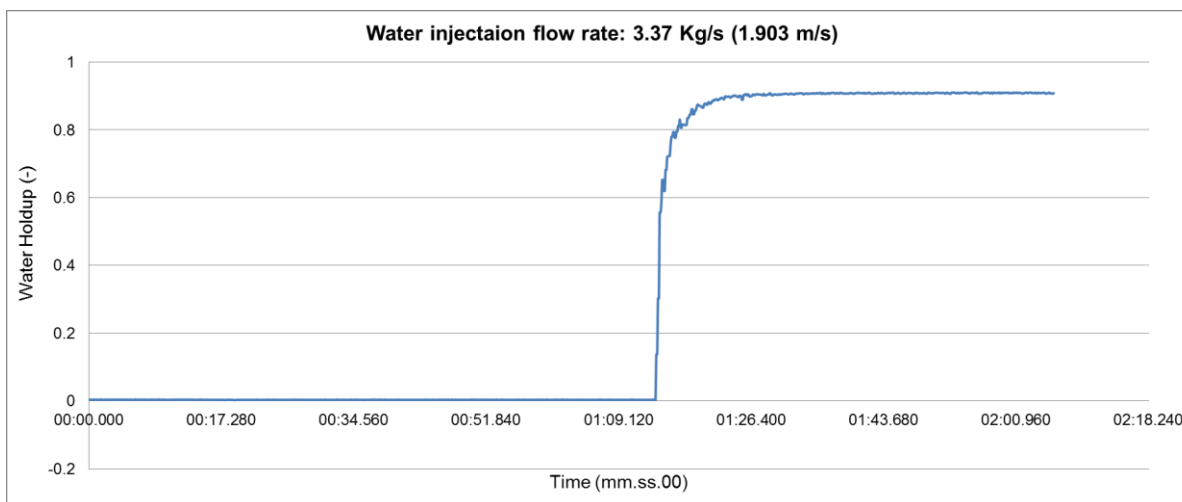
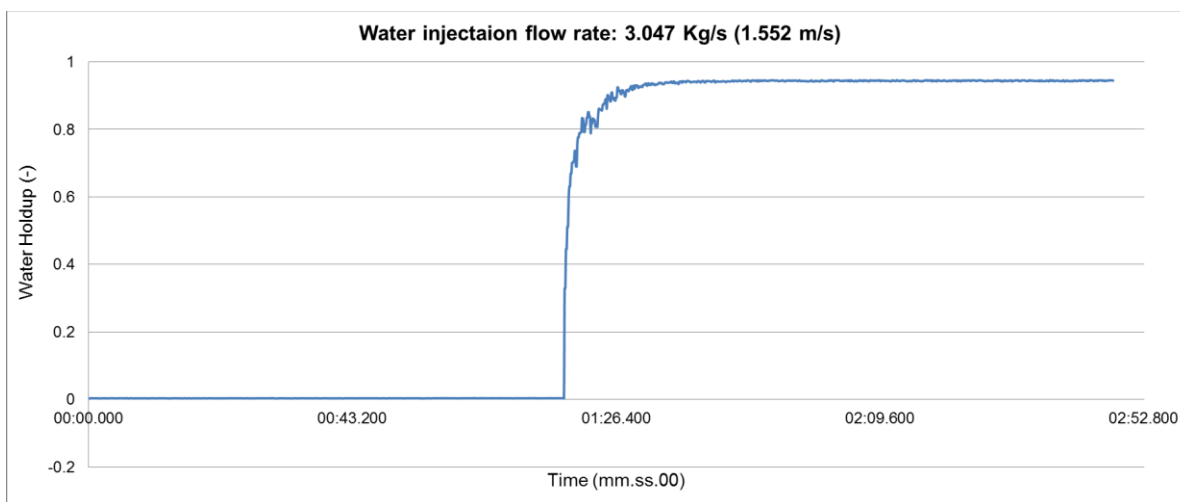
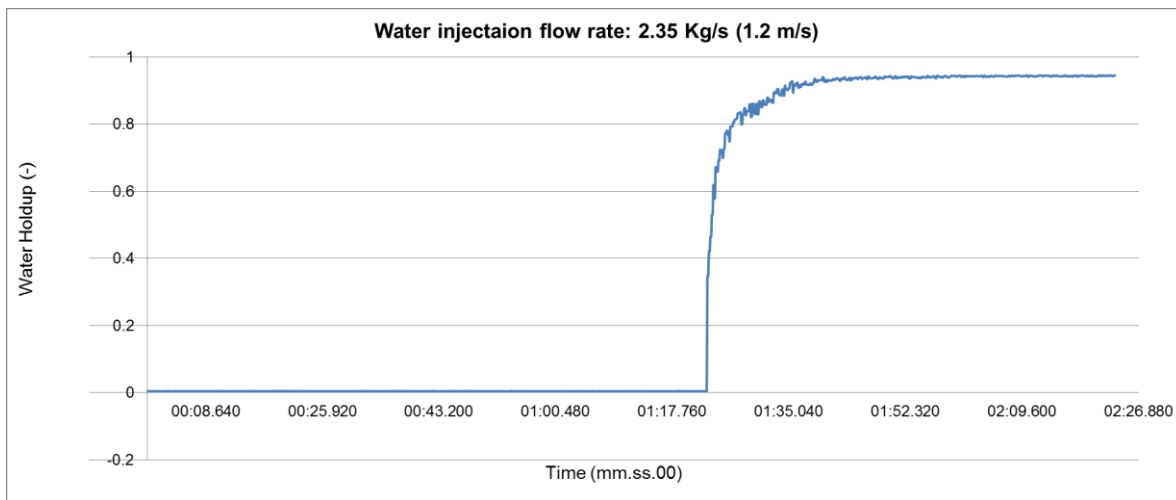


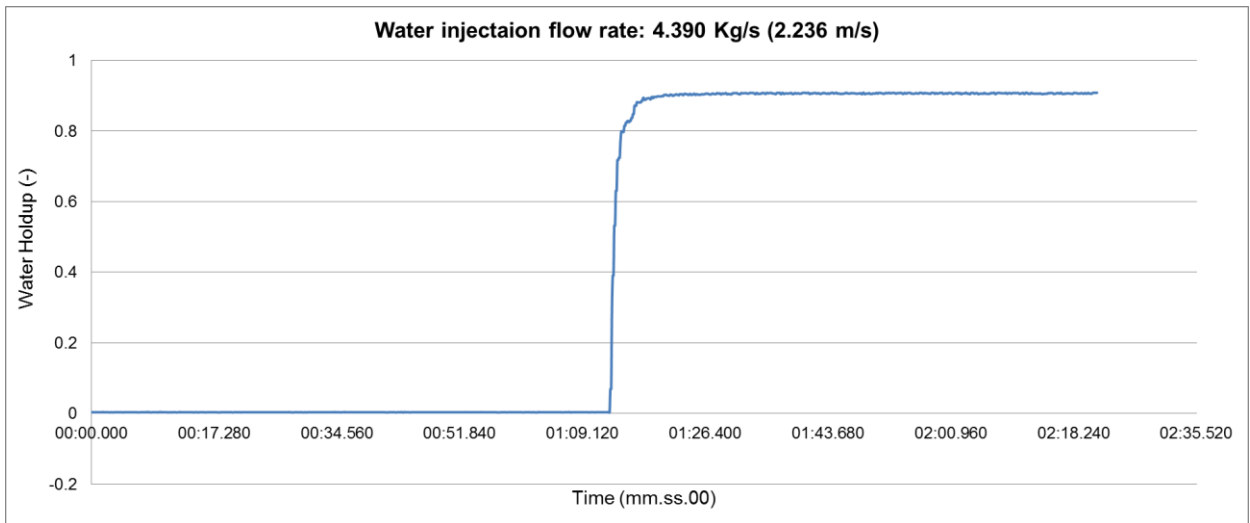


Appendix F

All graphs with different mass flow rate are represented in this section. All data are relevant to oil-water front experiments.

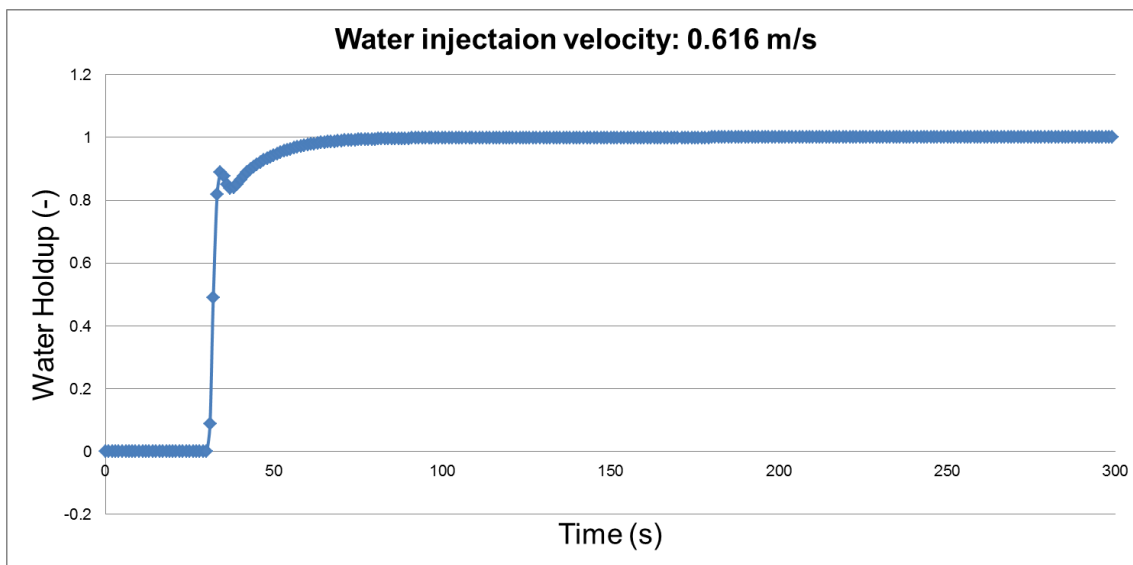
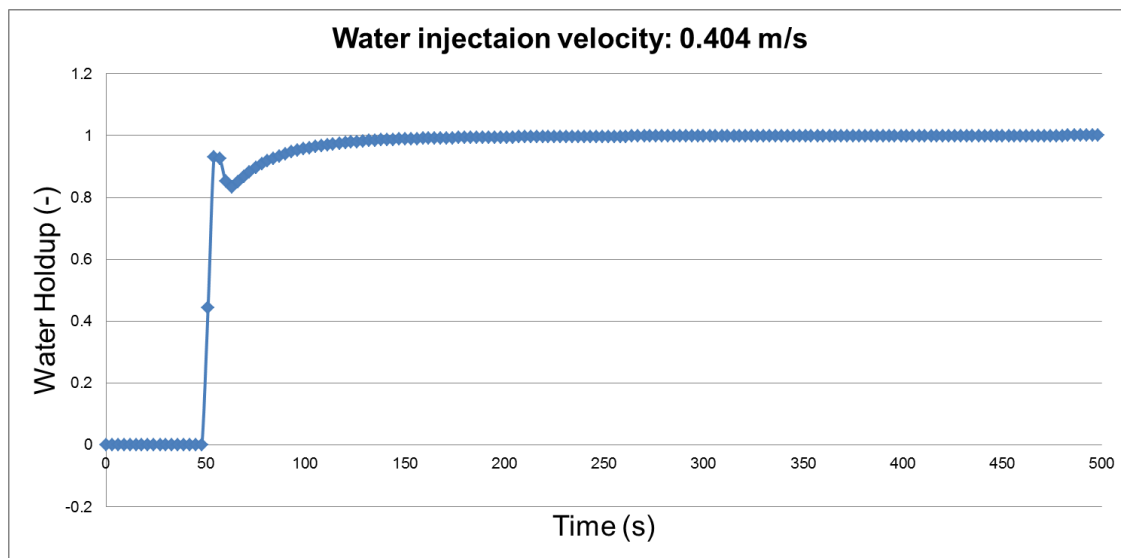


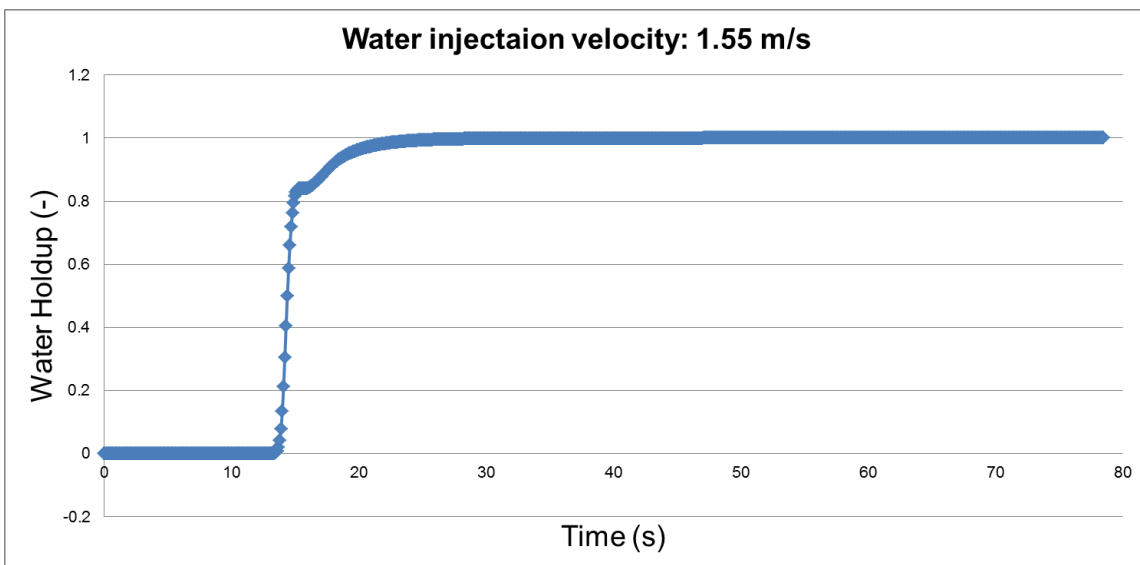
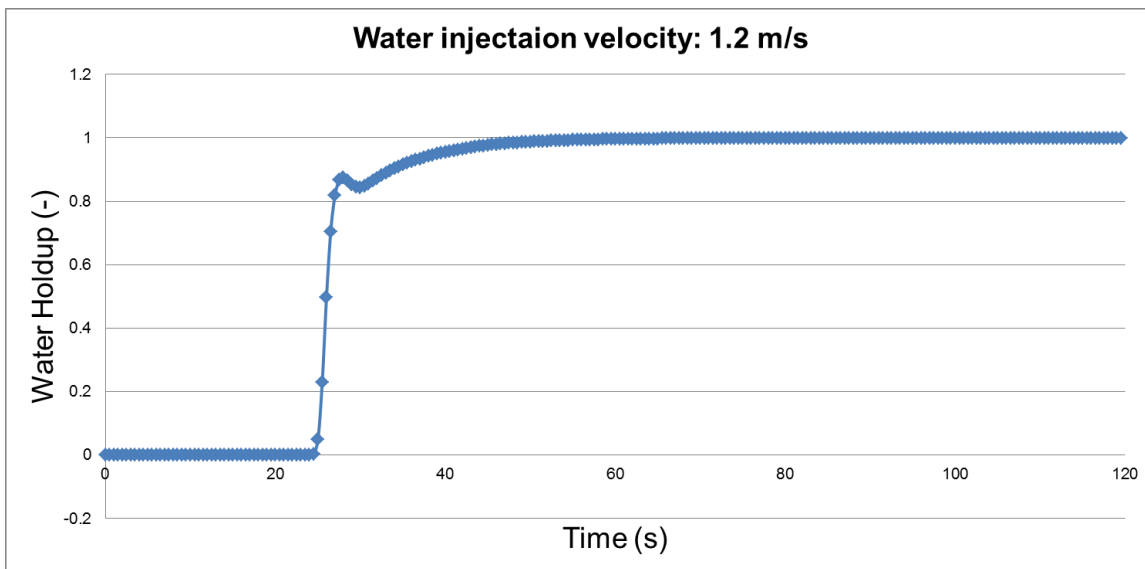
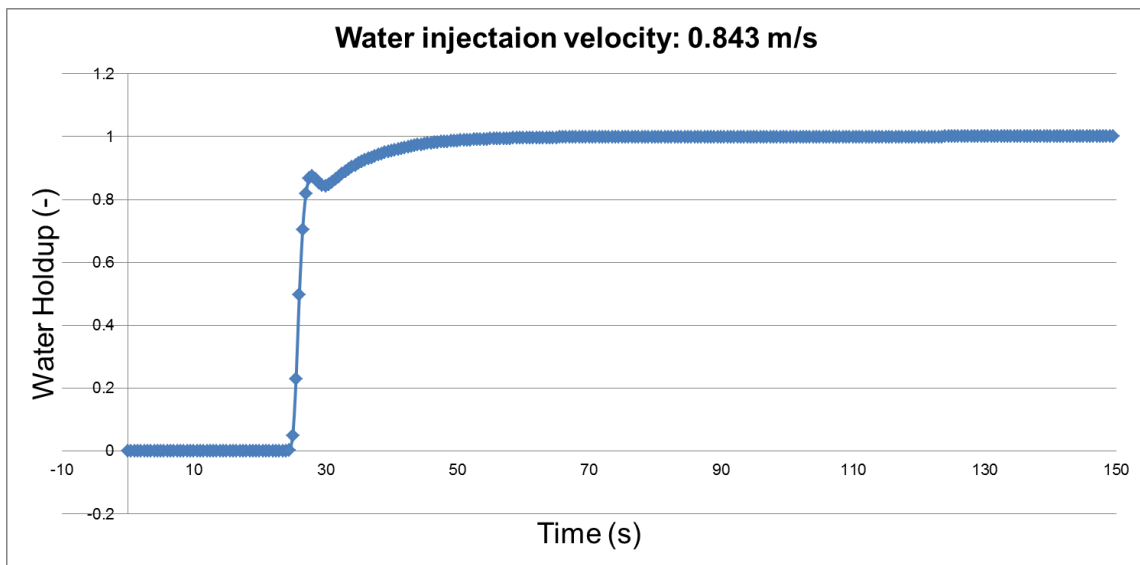


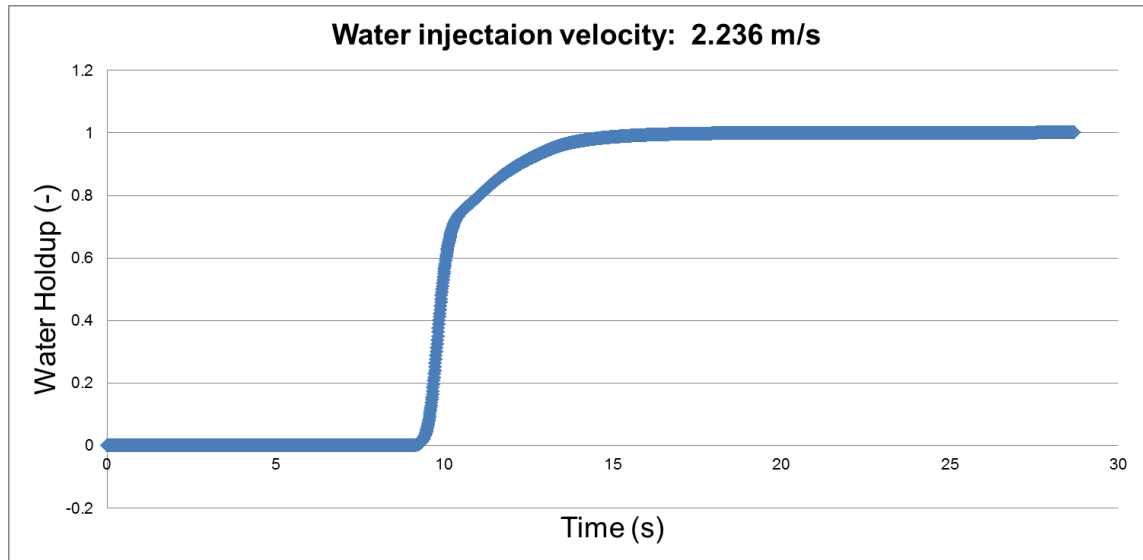
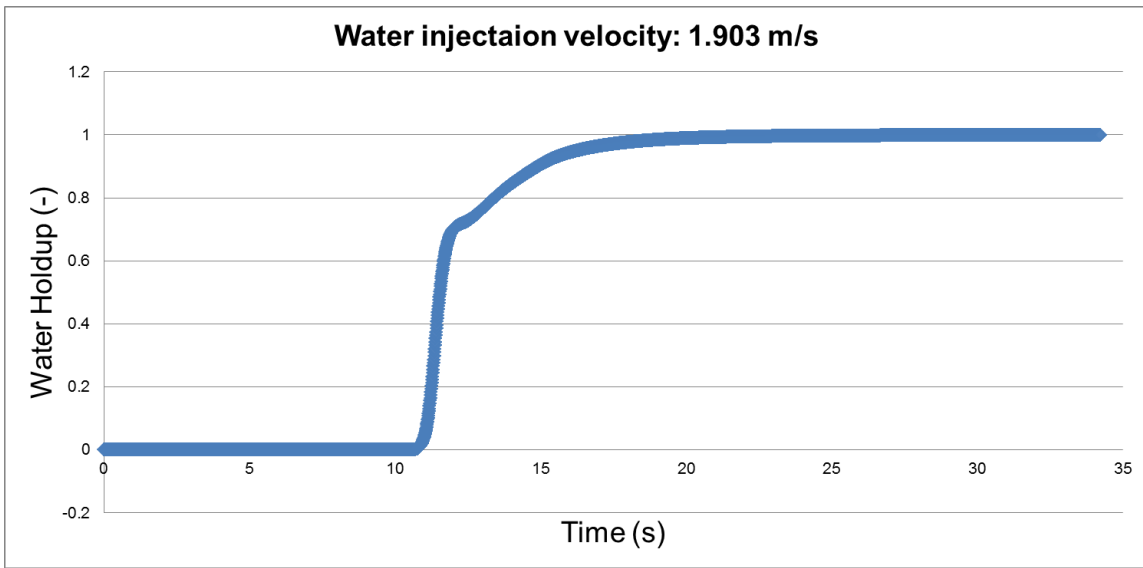


Appendix G

All graphs with different mass flow rate are represented in this section. All data are relevant to oil-water front simulation.







Appendix H

Pipe geometry is listed in details at **Table 0-3**.

Table 0-3: Pipe simulation geometry

X[m]	Y[m]	Z[m]	Diameter[m]	Roughness[m]	Temperature[°C]
0.00	0	0.00	0.05	1.00E-07	15
0.50	0	0.00	0.05	1.00E-07	15
0.59	0	0.01	0.05	1.00E-07	15
0.67	0	0.03	0.05	1.00E-07	15
0.75	0	0.07	0.05	1.00E-07	15
0.82	0	0.12	0.05	1.00E-07	15
0.88	0	0.18	0.05	1.00E-07	15
0.93	0	0.25	0.05	1.00E-07	15
0.97	0	0.33	0.05	1.00E-07	15
0.99	0	0.41	0.05	1.00E-07	15
1.00	0	0.50	0.05	1.00E-07	15
1.00	0	2.00	0.05	1.00E-07	15
1.01	0	2.07	0.05	1.00E-07	15
1.02	0	2.14	0.05	1.00E-07	15
1.05	0	2.20	0.05	1.00E-07	15
1.09	0	2.26	0.05	1.00E-07	15
1.14	0	2.31	0.05	1.00E-07	15
1.20	0	2.35	0.05	1.00E-07	15
1.26	0	2.38	0.05	1.00E-07	15
1.33	0	2.39	0.05	1.00E-07	15
1.40	0	2.40	0.05	1.00E-07	15
1.47	0	2.39	0.05	1.00E-07	15
1.54	0	2.38	0.05	1.00E-07	15
1.60	0	2.35	0.05	1.00E-07	15
1.66	0	2.31	0.05	1.00E-07	15
1.71	0	2.26	0.05	1.00E-07	15
1.75	0	2.20	0.05	1.00E-07	15
1.78	0	2.14	0.05	1.00E-07	15
1.79	0	2.07	0.05	1.00E-07	15
1.80	0	2.00	0.05	1.00E-07	15
1.80	0	1.00	0.05	1.00E-07	15
1.80	0	0.50	0.05	1.00E-07	15
1.81	0	0.41	0.05	1.00E-07	15
1.83	0	0.33	0.05	1.00E-07	15
1.87	0	0.25	0.05	1.00E-07	15
1.92	0	0.18	0.05	1.00E-07	15
1.98	0	0.12	0.05	1.00E-07	15
2.05	0	0.07	0.05	1.00E-07	15
2.13	0	0.03	0.05	1.00E-07	15
2.21	0	0.01	0.05	1.00E-07	15
2.30	0	0.00	0.05	1.00E-07	15
6.90	0	0.00	0.05	1.00E-07	15
6.99	0	0.01	0.05	1.00E-07	15
7.07	0	0.03	0.05	1.00E-07	15
7.15	0	0.07	0.05	1.00E-07	15
7.22	0	0.12	0.05	1.00E-07	15
7.28	0	0.18	0.05	1.00E-07	15
7.33	0	0.25	0.05	1.00E-07	15
7.37	0	0.33	0.05	1.00E-07	15
7.39	0	0.41	0.05	1.00E-07	15
7.40	0	0.50	0.05	1.00E-07	15

X[m]	Y[m]	Z[m]	Diameter[m]	Roughness[m]	Temperature[°C]
7.40	0	2.00	0.05	1.00E-07	15
7.41	0	2.07	0.05	1.00E-07	15
7.42	0	2.14	0.05	1.00E-07	15
7.45	0	2.20	0.05	1.00E-07	15
7.49	0	2.26	0.05	1.00E-07	15
7.54	0	2.31	0.05	1.00E-07	15
7.60	0	2.35	0.05	1.00E-07	15
7.66	0	2.38	0.05	1.00E-07	15
7.73	0	2.39	0.05	1.00E-07	15
7.80	0	2.40	0.05	1.00E-07	15
7.87	0	2.39	0.05	1.00E-07	15
7.94	0	2.38	0.05	1.00E-07	15
8.00	0	2.35	0.05	1.00E-07	15
8.06	0	2.31	0.05	1.00E-07	15
8.11	0	2.26	0.05	1.00E-07	15
8.15	0	2.20	0.05	1.00E-07	15
8.18	0	2.14	0.05	1.00E-07	15
8.19	0	2.07	0.05	1.00E-07	15
8.20	0	2.00	0.05	1.00E-07	15
8.20	0	0.50	0.05	1.00E-07	15
8.21	0	0.41	0.05	1.00E-07	15
8.23	0	0.33	0.05	1.00E-07	15
8.27	0	0.25	0.05	1.00E-07	15
8.32	0	0.18	0.05	1.00E-07	15
8.38	0	0.12	0.05	1.00E-07	15
8.45	0	0.07	0.05	1.00E-07	15
8.53	0	0.03	0.05	1.00E-07	15
8.61	0	0.01	0.05	1.00E-07	15
8.70	0	0.00	0.05	1.00E-07	15
17.20	0	0.00	0.05	1.00E-07	15